

# Characterisation of On-Site Sanitation Material and Products: VIP Latrines and Pour-Flush Toilets

## *VOLUME 2: LADEPA*

Report to the  
**Water Research Commission**

by

**Pollution Research Group  
University of KwaZulu-Natal**

List of authors:

Simon Mirara (M.Eng student)

Anusha Singh (PhD student)

Santiago Septien Stringel, PhD

Konstantina Velkushanova, PhD

Chris Buckley (Professor)

WRC Report No. 2137/2/18

ISBN 978-0-6392-0045-3

October 2018



**Obtainable from**

Water Research Commission  
Private Bag X03  
Gezina, 0031

[orders@wrc.org.za](mailto:orders@wrc.org.za) or download from [www.wrc.org.za](http://www.wrc.org.za)

The publication of this report emanates from a project entitled *Characterisation of On-Site Sanitation Material and Products: VIP Latrines and Pour-Flush Toilets* (WRC Project No. K5/2137).

This report form part of a series of two reports. The other report is *Characterisation of faecal sludge from pour-flush latrines* (WRC Report No. 2137/1/18).

**DISCLAIMER**

This report has been reviewed by the Water Research Commission (WRC) and approved for publication. Approval does not signify that the contents necessarily reflect the views and policies of the WRC, nor does mention of trade names or commercial products constitute endorsement or recommendation for use.

## EXECUTIVE SUMMARY

When eThekweni Municipality was established in 1999, over 60 000 *Ventilated Improved Pit* (VIP) latrines were inherited from the incorporated local entities. In 2009, the municipality set out to empty over 35 000 VIP latrines, which were already full. One of the challenges from this operation was the disposal of the sludge in an environmentally safe way. The initial idea was to dispose of the sludge in wastewater treatment plants but the first trials caused overloading and dysfunction of the treatment plant. Consequently, the municipality had to seek alternative solutions for the disposal of faecal sludge. This led to the concept of the **LA**trine **DE**hydration and **PA**steurisation (LaDePa) machine, manufactured by Particle Separation System (PSS). This machine is used to process the faecal sludge that was removed from latrines into dry and pasteurised pellets, which can be used as a soil conditioner or fertiliser, or which could be combusted as a fuel. In the developed technology, the pellets are pasteurised and dried using a combination convective and infrared radiation heating.

A LaDePa machine small-scale prototype was installed in the Pollution Research Group (PRG) laboratory, situated at the University of KwaZulu-Natal, Durban. Its objective was to understand better the drying process in the LaDePa process and optimise the operation of the full-scale machine. The aim of this work was to characterise the LaDePa process using the laboratory-scale machine. It was envisaged that this would ultimately lead to the determination of the optimum operating conditions for drying and pasteurisation.

The research focussed on two main aspects. The first one corresponds to the study of the drying behaviour of the faecal sludge in the LaDePa, which was done by measuring the moisture, volatile matter and ash content at different heating intensities and residence times. The major findings for this aspect of the study were:

- At high *Medium InfraRed* (MIR) emitter intensity (temperatures higher than 200°C), drying occurs the fastest and it is the most efficient. However, this was coupled with a considerable risk of undesirable thermal degradation and burning of the pellets. At MIR emitter intensity (temperatures between 100°C and 200°C), the risk of thermal degradation is avoided but drying takes longer. Under these conditions, a residence time of approximately 20 minutes is necessary to reduce the moisture content to 20%. At low MIR intensity (temperatures lower than 100°C), drying is too slow. In all cases, complete pasteurisation is insured in less than 8 minutes.
- The recommended MIR emitter intensity should be the highest one possible without thermal degradation of the pellets. For future work, it is important to determine the temperature and corresponding intensity at which thermal degradation first occurs.
- Minimising the distance between the emitters and the conveyer belt would lead to energy saving due to a lower MIR intensity required to achieve the targeted moisture content and complete pasteurisation.
- Decreasing the pellet size leads to faster drying and a more efficient process.
- Drying rate is slightly faster for faecal sludge without pre-treatment than for a pre-treated sample.
- Drying will be faster by increasing the air flowrate in the heating zone as it will lead to a better evacuation of the evaporated moisture from the surface of the pellets to the environment.

However, the air should be heated in order to avoid a cooling effect on particle surface, which has a negative effect on drying rate.

- From a phenomenological point of view, drying occurs in the constant rate period in the early stage and then pellets remain isothermal at the moisture evaporation temperature. After removal of approximately half of the moisture, the drying rate declines, indicating that the pellet surface is fully or partially dried. Therefore, the temperature at the surface increases and becomes considerably higher than at the core. If the heating flux from MIR emitters is too high, the dried surface can be thermally degraded while the core continues to dry.

The second aspect is the biological, chemical and physical characteristics of the processed pellets. Indeed, the analysis of the *Ascaris* content of the processed pellets, a hardy pathogen indicator, was performed in order to determine the extent of pasteurisation. The chemical analysis in the major nutrients, namely nitrogen, phosphorus and potassium, was evaluated in order to assess the pellet quality for agriculture purposes. The calorific value, thermal conductivity and heat capacity was also determined in order to evaluate the use of the pellets as a biofuel. The findings were summarised as follows:

- Drying provokes some chemical and physical modifications in the pellets: a decrease of the concentration of the soluble nitrogenous compounds, suggesting chemical changes of the nitrogen form in the sample; a decrease in the thermal conductivity and heat capacity, leading to globally a slight increase of the thermal diffusivity. After removing 80% of the initial moisture, these thermal properties attain a stable value.
- The dried pellets present an interesting nutrient composition in terms of macronutrients, Phosphorus (P) and Potassium (K), and micronutrients, Magnesium (Mg) and Calcium (Ca). If used for agricultural purposes, most of the phosphorous will be slowly released in the soil. A considerable part of the potassium, magnesium and calcium could be expected to be fast released in the soil, as these compounds are very soluble in water. The dried pellets would rapidly release some nitrogen, mainly as ammonium and nitrites. These forms are not the most optimal for assimilation by the plants, compared to nitrates, but they can be converted into the latter one by soil microbial activity.
- The use of dried pellets as a biofuel is a potentially interesting alternative, because of the relatively high calorific value and good thermal diffusivity of the material.

In a more general context, this work can be of great interest for the scientific community from the sanitation sector, as of the date of publishing, no works in literature exist about the thermal drying of faecal sludge and its applications. In order to ensure simplicity of understanding the research process and outcomes, the studies of both *Pour Flush (Volume 1)* and *LaDePa (Volume 2)* are presented as two separate volumes within Research Project K5/2137. This report presents the latter (Volume 2).

## ACKNOWLEDGMENTS

- Water Research Commission (WRC) for its funding, special thanks to Mr. Jay Bhagwan (Chair: 2012-2013) and Dr. Sudhir Pillay (Chair: 2014-2015).
- eThekweni Water Services (EWS) for its support, special thanks to Mr. Teddy Gounden, Mr. Dave Wilson and Mr. John Harrison.
- Particle System Separation (PSS) for its support, special thanks to Mr. Rein Buisman.
- Professor Alfred Odindo from the Agriculture Department of the University of KwaZulu-Natal.
- Reference Group Members for Research project K5/2137.
- Students involved in the research. A full list of researchers has been included in Chapter 7.
- Technical and support staff from the Pollution Research Group (PRG) from the University of KwaZulu-Natal for its involvement, special thanks to Ms. Susan Mercer, Ms. Merlien Reddy and Mr. Kenneth Jack.

This page was deliberately left blank

## TABLE OF CONTENTS

<b>EXECUTIVE SUMMARY</b> .....	<b>i</b>
<b>ACKNOWLEDGMENTS</b> .....	<b>iii</b>
<b>TABLE OF CONTENTS</b> .....	<b>v</b>
<b>LIST OF FIGURES</b> .....	<b>vii</b>
<b>LIST OF TABLES</b> .....	<b>ix</b>
<b>NOMENCLATURE</b> .....	<b>x</b>
<b>1. BACKGROUND</b> .....	<b>1</b>
<b>2. MATERIALS AND METHODS</b> .....	<b>4</b>
<b>2.1 SAMPLING FAECAL SLUDGE</b> .....	<b>4</b>
<b>2.2 LABORATORY-SCALE LADEPA</b> .....	<b>4</b>
<b>2.3 EXPERIMENTAL PROCEDURE</b> .....	<b>5</b>
2.3.1 Extrusion of pellets.....	5
2.3.2 Experimental conditions in laboratory-scale LaDePa .....	6
2.3.3 Measurement of temperature within the pellets.....	7
2.3.4 Characterisation of the faecal sludge and processed pellets.....	7
<b>2.4 ERROR ANALYSIS</b> .....	<b>8</b>
<b>3. RESULTS AND DISCUSSION</b> .....	<b>9</b>
<b>3.1 PARAMETERS AFFECTING DRYING PROCESS IN LADEPA</b> .....	<b>9</b>
3.1.1 Drying temperature.....	9
3.1.1.1 Effect of MIR intensity at constant emitter height.....	9
3.1.1.2 Effect of emitter height at constant temperature .....	11
3.1.2 Airflow around the pellet .....	12
3.1.2.1 Effect of airflow rate at constant MIR intensity .....	12
3.1.2.2 Effect of airflow rate at constant drying temperature .....	12
3.1.3 Effect of the pellet size.....	13
3.1.4 Bulking pre-treatment of sample .....	14
<b>3.2 DRYING PROCESS</b> .....	<b>15</b>
3.2.1 Temperature within the pellets during drying.....	15
3.2.2 Kinetic study of pellets drying.....	16
<b>3.3 EFFICIENCY OF THE PROCESS</b> .....	<b>18</b>
3.3.1 Drying efficiency.....	18
3.3.1.1 Drying efficiency as a function of MIR intensity.....	18
3.3.1.2 Drying efficiency as a function of MIR height at fixed drying temperature .....	19
3.3.1.3 Drying efficiency as a function of the air flow rate .....	19
3.3.1.4 Drying efficiency as a function of pellet size .....	21
3.3.1.5 Summary .....	21
3.3.2 Pasteurisation efficiency .....	21
<b>3.4 CHARACTERISATION OF PELLETS</b> .....	<b>22</b>
3.4.1 Chemical analysis .....	22

3.4.1.1	Elemental analysis .....	22
3.4.1.2	Molecular compounds .....	24
3.4.1.3	Summary .....	25
3.4.2	Thermal analysis.....	26
3.4.2.1	Calorific value .....	26
3.4.2.2	Thermal conductivity.....	27
3.4.2.3	Heat capacity .....	28
3.4.2.4	Thermal diffusivity.....	29
3.4.2.5	Summary .....	30
<b>4.</b>	<b>CONCLUSIONS.....</b>	<b>31</b>
<b>5.</b>	<b>IMPROVEMENTS IN THE FULL SCALE LADEPA.....</b>	<b>32</b>
<b>5.1</b>	<b>THERMAL AND MASS TRANSFER ANALYSIS.....</b>	<b>32</b>
5.1.1	Heat and mass transfer calculations .....	32
5.1.1.1	Convection heat transfer calculations.....	32
5.1.1.2	Conduction heat transfer calculations .....	33
5.1.1.3	Radiative heat transfer calculations .....	34
5.1.1.4	Convective mass transfer calculations .....	36
5.1.2	Parameters used for the calculations .....	36
5.1.2.1	Air and pellets physical properties .....	36
5.1.2.2	LaDePa dimensions .....	37
5.1.2.3	LaDePa operating conditions .....	37
5.1.3	Results obtained from the calculations.....	37
5.1.3.1	Case 1 .....	37
5.1.3.2	Case 2 .....	39
5.1.3.3	Case 3 .....	41
5.1.4	Summary .....	41
<b>5.2</b>	<b>PELLET CONTAMINATION BY THE EXHAUST GAS FROM THE DIESEL ENGINE.....</b>	<b>42</b>
<b>5.3</b>	<b>IMPROVEMENT OF LADEPA DESIGN .....</b>	<b>43</b>
<b>6.</b>	<b>LIST OF PUBLICATIONS .....</b>	<b>46</b>
<b>7.</b>	<b>CAPACITY BUILDING.....</b>	<b>47</b>
<b>8.</b>	<b>REFERENCES.....</b>	<b>48</b>
<b>APPENDIX 1:</b>	<b>RHEOLOGICAL CHARACTERISATION OF THE VIP FEACAL SLUDGE.....</b>	<b>50</b>
<b>APPENDIX 2:</b>	<b>TEMPERATURE MEASUREMENT DATA.....</b>	<b>51</b>
<b>APPENDIX 3:</b>	<b>EFFECT OF PARTICLE SIZE AND AIR FLOWRATE ON THE POTASSIUM AND PHOSPHOROUS COMPOSITION OF THE PELLETS .....</b>	<b>52</b>
<b>APPENDIX 4:</b>	<b>EFFECT OF PARTICLE SIZE AND AIR FLOWRATE ON THE CALORIFIC VALUE .....</b>	<b>54</b>

## LIST OF FIGURES

Figure 1. Front view of the full-scale LaDePa.....	1
Figure 2. Back view of the full-scale LaDePa.....	2
Figure 3. Scheme of the full-scale LaDePa .....	2
Figure 4. Laboratory-scale LaDePa .....	4
Figure 5. LaDePa schematic.....	5
Figure 6. Capillary extruder .....	6
Figure 7. Thermocouple position for temperature measurements in laboratory-scale LaDePa.....	6
Figure 8. Drying curves at varying MIR intensity, at constant emitter height (11.5 cm), for the 8 mm pellets ....	10
Figure 9. Volatile solids (VS) and ash content at varying intensity and residence time, at constant emitter height (11.5 cm), for the 8 mm pellets .....	10
Figure 10. Drying curves at varying heights of the MIR emitter above the belt, at constant temperature (~ 140°C) and MIR intensity, for the 8 mm pellets .....	11
Figure 11. Drying curves for different airflow rates at constant MIR intensity (50%), for the 8 mm pellets .....	12
Figure 12. Drying curves for different airflow rate at constant drying temperature (~ 140°C), for the 8 mm pellets .....	13
Figure 13. Drying curves for different pellet diameters .....	14
Figure 14. Drying curves for different samples, for the 8 mm pellets .....	14
Figure 15. Temperature measured in the 8 and 14 mm pellets versus the distance conveyed, during experiments at 50% MIR intensity and residence time around 20-25 minutes .....	15
Figure 16. Moisture content in dry basis versus residence time at different MIR intensities for the 8 mm pellets (A) and for different pellet diameters at 50% of MIR intensity (B).....	17
Figure 17. Moisture removal versus energy consumption for different MIR intensities, at fixed emitter height (11.5 cm), for the 8 mm pellets.....	18
Figure 18. Moisture removal versus energy consumption for different emitters heights, at fixed temperature (~ 140°C) and variable MIR intensities, for the 8 mm pellets .....	19
Figure 19. Moisture removal versus energy consumption as a function of the air flowrate (related to the suction valve opening degree), for the 8 mm pellets.....	20
Figure 20. Moisture removed versus energy consumption for pellets of different sizes.....	21
Figure 21. Concentration of C and N in the 8 mm pellets processed at different residence times and MIR intensities.....	23
Figure 22. Concentration of P and K in the 8 mm pellets processed at different residence times and MIR intensities.....	23
Figure 23. Concentration of Mg and Ca in the 8 mm pellets processed at different residence times and MIR intensities.....	24
Figure 24. Calorific value for the 8 mm pellets at different residence times and MIR intensities.....	26
Figure 25. Thermal conductivity for the 8 mm pellets at different residence times and MIR intensities.....	27
Figure 26. Thermal conductivity versus moisture content from the 8 mm pellets during processing at different MIR intensities .....	28
Figure 27. heat capacity for the 8 mm pellets at different residence times and MIR intensities.....	28
Figure 28. Heat capacity versus moisture content from the 8 mm pellets during processing at different MIR intensities.....	29
Figure 29. Thermal diffusivity for the 8 mm pellets for the 8 mm pellets at different residence times and MIR intensities .....	30
Figure 30. Equations for the calculation of the view factor between two parallel rectangular surfaces .....	35
Figure 31. Temperature of the fresh and dry faecal sludge at the surface (A) and at the centre (B) .....	38
Figure 32. View of factor versus the distance between the MIR and the conveyer belt .....	39

Figure 33. Temperature at the pellet surface in the MIR heating zone – (A) carrier gas at ambient TEMPERATURE; (B) carrier gas pre-heated to 400°C; (C) carrier gas pre-heated to 400°C and suction section area reduced by a factor of 5 ..... 40

Figure 34. Typical diesel composition [21, 22] ..... 42

Figure 35. Typical exhaust gas composition from Diesel combustion [23] ..... 43

Figure 36. Diagram flow sheet of the improved LaDePa design ..... 45

Figure A.1. Rheological curves for the raw faecal sludge with and without the addition of sawdust ..... 50

Figure B.1. Temperature measured under the first MIR emitter at different MIR intensities and emitter heights ..... 51

Figure B.2. Temperature measured under the second MIR emitter at different MIR intensities and emitter heights ..... 51

Figure C.1. Concentration of K in the 8 mm, 10 mm, 12 mm and 14 mm pellets processed at different residence times ..... 52

Figure C.2. Concentration of P in the 8 mm, 10 mm, 12 mm and 14 mm pellets processed at different residence times ..... 53

Figure C.3. Concentration of K in the 8 mm pellets processed at different air flowrates and residence times .... 53

Figure D.1. Heat capacity of the 8 mm, 10 mm, 12 mm and 14 mm pellets processed at different residence times ..... 54

## LIST OF TABLES

<i>Table 1. Comparison between the laboratory-scale and full-scale LaDePa.....</i>	<i>4</i>
<i>Table 2. Summary of conditions under investigation .....</i>	<i>7</i>
<i>Table 3. Analysis to be carried out on the faecal sludge and pellets processed in the laboratory-scale LaDePa ...</i>	<i>8</i>
<i>Table 4. Corresponding MIR intensities and temperatures .....</i>	<i>9</i>
<i>Table 5. Correlation between the MIR intensity and the power consumed.....</i>	<i>18</i>
<i>Table 6. Ascaris egg concentration for various samples processed at different conditions .....</i>	<i>22</i>
<i>Table 7. Order of magnitude of the concentration of ammonia, nitrates, nitrites and phosphates in the 8 mm pellets during drying .....</i>	<i>25</i>
<i>Table 8. Physical properties of air at 20°C and 400°C.....</i>	<i>36</i>
<i>Table 9. Physical properties of the raw and processed faecal sludge.....</i>	<i>37</i>
<i>Table 10. Dimensions of the different sections of the full scale LaDePa.....</i>	<i>37</i>

## NOMENCLATURE

### Acronyms

IR	InfraRed
LaDePa	Latrine Dehydration Pasteurisation
MIR	Medium InfraRed
PRG	Pollution Research Group
PSS	Particle System Separation
UKZN	University of KwaZulu-Natal
VIP	Ventilated Improved Pit
WRC	Water Research Commission

### Chemical nomenclature

C	Carbon
Ca	Calcium
K	Potassium
Mg	Magnesium
N	Nitrogen
NH <sub>4</sub> <sup>+</sup>	Ammonia
NO <sub>2</sub> <sup>-</sup>	Nitrites
NO <sub>3</sub> <sup>-</sup>	Nitrates
P	Phosphorous
PO <sub>4</sub> <sup>-3</sup>	Phosphates
S	Sulphur

## 1. BACKGROUND

When eThekweni Municipality was established in 1999, over 60 000 *Ventilated Improved Pit* (VIP) latrines were inherited from the incorporated local entities. In 2009, the municipality set out to empty over 35 000 VIP latrines, which were already full. One of the challenges from this operation was the disposal of the faecal sludge that had accumulated in the latrines in an environmentally safe way. The initial idea was to dispose of the sludge in wastewater treatment plants but this caused overloading of the treatment plants. Consequently, the municipality had to seek an alternative solution to manage faecal sludges. This led to the concept of the *LAtrine DEhydration and PAsteurisation* (LaDePa) machine, manufactured by *Particle Separation System* (PSS). The machine was manufactured and used to process the collected faecal sludge from pit latrines and process it into dried and pasteurised pellets, which can be used as a soil conditioner or fertiliser, or which could be combusted as a fuel. The LaDePa process involves pellet pasteurisation and drying through the combination of convective and *Medium Infrared Radiation* (MIR) heating. The heat pasteurises the faecal sludge by destroying the vital structure of microorganisms, viruses and parasites, and leads to the evaporation of the moisture. Infrared drying has been widely used in several industrial sectors [1]: pulp and paper industry, textile industry, minerals drying, polymer solutions, and food industry. It is well known that infrared drying is a more efficient than convective methods because of a more depth penetration of the heat within the solid. Better results were obtained with medium infrared emitters than low or high infrared emitters due to a higher heat absorption in that wavelength range [2,3].

The LaDePa machine is located in the Tongaat wastewater treatment plan, 37 km north of Durban. Figure 1 and Figure 2 show photographs of the side views (front and back) of LaDePa, respectively. This process comprises an extrusion section and a drying and pasteurisation section. A diesel generator provides the electricity and heating necessary for processing the VIP sludge. The faecal sludge that is emptied from the VIP latrines is transported to site and stored in open air until LaDePa processing.



FIGURE 1. FRONT VIEW OF THE FULL-SCALE LADEPA



FIGURE 2. BACK VIEW OF THE FULL-SCALE LADEPA

Faecal sludge is fed onto a porous conveyer belt as cylindrical pellets, by using a screw extruder which also separates the detritus from the sludge. The pellets are then conveyed to the drying section. The latter consists of a pre-drying section, where the sludge is first dried using exhaust heat from a diesel engine, and the second section where the sludge is dried using successive medium wave infrared (MIR) emitters. Suction boxes under the moving belt draws hot air through the section, which assists in the drying of the pellets. The dried material is then discharged into the collection chute and bagged. The LaDePa process is schematised in Figure 3.

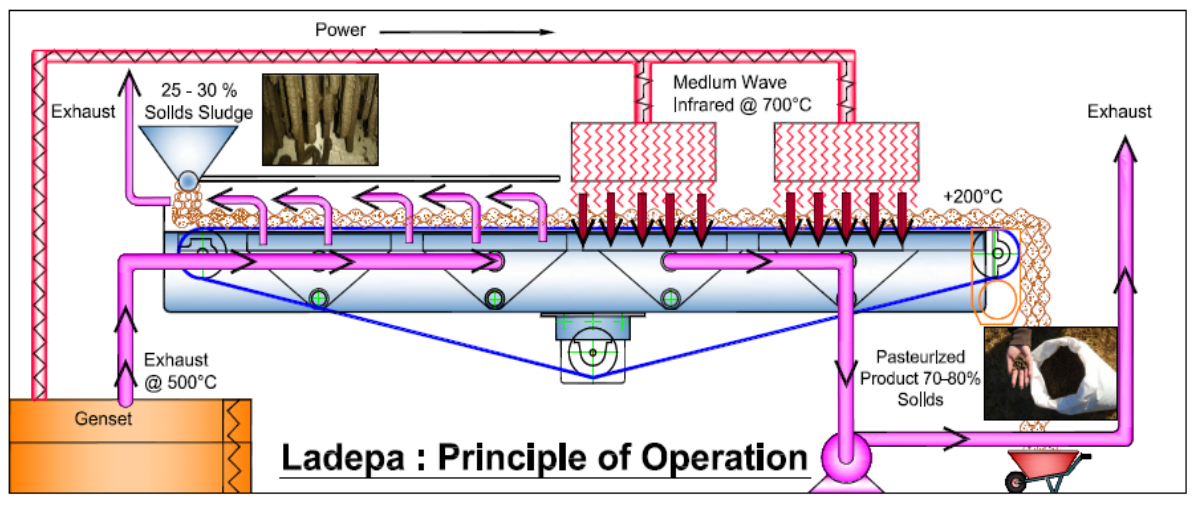


FIGURE 3. SCHEME OF THE FULL-SCALE LADEPA

The aim of this work is to characterise the LaDePa treatment processes using a laboratory-scale machine which has been installed in the laboratory of the Pollution Research Group (PRG), situated at the University of KwaZulu-Natal, Durban, South Africa. The objective of this prototype is to better understand the involved treatment processes in the LaDePa process and optimise the operation of the full-scale machine.

There are two main objectives of this research:

- To characterise the drying and pasteurisation behaviour of VIP faecal sludge in LaDePa machine.
- To determine the chemical and thermal characteristics of the processed pellets, in order to evaluate the use of the dried product for agricultural purposes or as a biofuel.

No research about the thermal drying of human faecal matter and its applications have been published in literature until now. Nonetheless, several publications can be found for similar material such as sewage sludge and cattle manure for different methods to *InfraRed* (IR) drying. Different aspects of manure drying have been explored for agriculture or animal feed application, among which drying times, disinfection, odours and nutrient content of the dried pellets [4-7]. Several authors [8-10] have explored the use of manure as a biofuel. Bennamoun and co-workers [11] reviewed different drying methods for sewage sludge and the kinetics behaviour as a function of the operating conditions and the application from which the sludge is issued. However, none of these studies deal with IR drying.

Faecal sludge IR drying and the valorisation of the dried product are then original research topics. IR drying has not been used for manure or sewage sludge.

Under this project (K5/2317: Volume 2), a number of deliverables have been submitted in relation to the LaDePa research:

- Deliverable 1: description of a protocol for laboratory drying tests using a convective dryer (which finally was not used for this study);
- Deliverable 2: description of the full scale LaDePa machine located in Tongaat;
- Deliverable 3: description of the experimental protocol for the characterisation of the raw faecal sludge;
- Deliverable 4: description of the experimental protocol for the characterisation of the pellets obtained from the laboratory-scale LaDePa;
- Deliverable 6: report presenting a bibliographic review on drying and extrusion, and preliminary results (extrusion tests using the screw extruder and the hand capillary extruder with synthetic sludge; temperature measurements in laboratory-scale LaDePa during operation);
- Deliverable 8: description of drying theory;
- Deliverable 9: final report of LaDePa presenting the experimental methodology, results obtained and conclusions from the project.

In the next Chapter, the Materials and Methods used for experiments are presented.

## 2. MATERIALS AND METHODS

This chapter has four subsections that details the sampling (**section 2.1**), the laboratory LaDePa prototype (**section 2.2**), the experimental programme (**section 2.3**) and the error analysis used in data interpretation (**section 2.4**).

### 2.1 SAMPLING FAECAL SLUDGE

Faecal sludge was sampled during the emptying of ventilated improved pit (VIP) latrines in different settlements in Durban metropolis. After collection, the samples were transported to the Pollution Research Group laboratory, where they were stored in a cold room at 4°C. Before the tests, the faecal sludge was sieved through 5.6 mm sieve in order to remove the non-faecal coarse particles and obtain a homogeneous texture.

### 2.2 LABORATORY-SCALE LADEPA

In order to study LaDePa process, a laboratory-scale prototype machine was installed in the Pollution Research Group (PRG) laboratory, as displayed in Figure 4. The laboratory-scale LaDePa is a replica of the full-scale machine with a size reduction of approximately 10:1. A comparison of the two LaDePa machines (full-scale and laboratory-scale) is provided in Table 1.



FIGURE 4. LABORATORY-SCALE LADEPA

TABLE 1. COMPARISON BETWEEN THE LABORATORY-SCALE AND FULL-SCALE LADEPA

Feature	Full-scale LaDePa (located at Tongaat)	Laboratory-scale LaDePa (located at the PRG laboratory)
<b>Belt width</b>	950 mm	250 mm
<b>Belt aperture opening</b>	300 µm	200 µm
<b>Heated width</b>	1350 mm	220 mm
<b>Heated length</b>	11,000 mm	880 mm
<b>MIR power</b>	3 emitters each 48kW	2 emitters each 3.7kW
<b>Blower power</b>	5.5kW	0.75kW

The operation of the laboratory-scale LaDePa is very similar to the full-scale machine. Pellets are formed by extrusion and are disposed onto the porous steel conveyer belt which transports the pellets into the heating zone. There, the pellets are exposed to heat in the form of thermal radiation from two medium infrared (MIR) emitters. The pellets leave the belt via a discharge chute. There are two vacuum chutes under the belt that pull the air through so that there is continuous movement of air, facilitating drying and ensuring that the evaporated moisture is removed. A schematic diagram of the laboratory-scale LaDePa is shown on Figure 5.

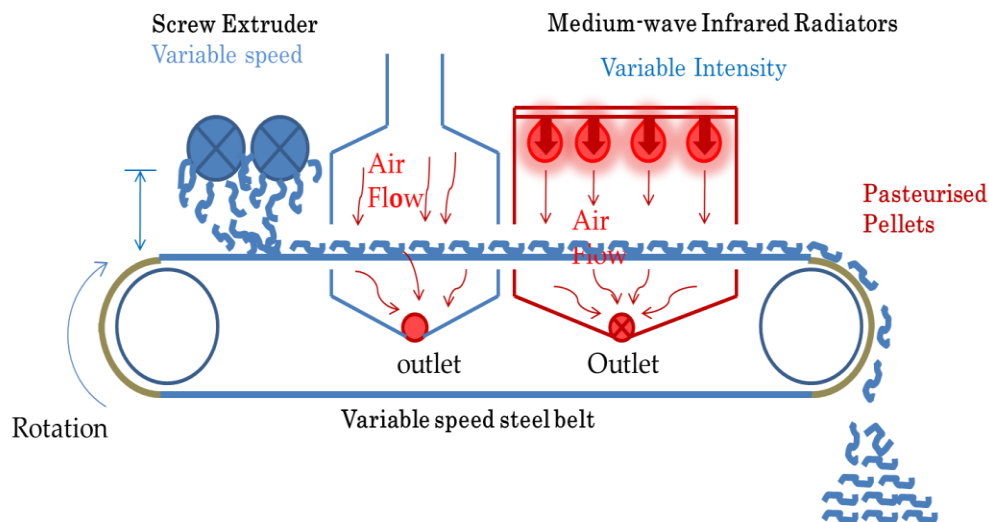


FIGURE 5. LADEPA SCHEMATIC

## 2.3 EXPERIMENTAL PROCEDURE

### 2.3.1 EXTRUSION OF PELLETS

Initially, extrusion was planned to be performed with a screw extruder to simulate extrusion in LaDePa process. However, during preliminary tests, the operation of the extruder was problematic as it tended to be completely clogged after a few minutes. Some technical modifications on the extruder, as well as efforts to understand and limit the clogging, were unsuccessful. Hence, the screw extruder was replaced by a hand held capillary extruder, which is much simpler to use and presents no significant problems of clogging. In contrast, it does not allow high loads of pellets on the belt.

The hand held capillary extruder consists of a tube with an air inlet connected to a pressure line on one side, and a hole with a diameter of 14 mm on the other side. For each run, the capillary extruder is filled with faecal sludge. After opening the air inlet valve, the compressed air forces the faecal sludge out through the hole on the opposite side. Pellets with a diameter of 14 mm are then produced. The size of the pellets can be varied by inserting plates of different sizes on the outlet of the extruder.

Sawdust was added to the faecal sludge to produce pellets that held their shape. Without the addition of sawdust, the pellets tend to get flat after extrusion because of a more predominant liquid behaviour than plastic. Indeed, the sawdust increases the plasticity of the faecal sludge. A photograph of the capillary extruder is shown in Figure 6.



FIGURE 6. CAPILLARY EXTRUDER

### 2.3.2 EXPERIMENTAL CONDITIONS IN LABORATORY-SCALE LADEPA

Experiments on the laboratory-scale LaDePa were conducted by varying the residence time, temperature and airflow rate circulating in the drying zone. The residence time was controlled by fixing the speed of the belt at a given value. The temperature was controlled by adjusting the emitters MIR intensity and/ or the distance with respect to the belt. Temperature was measured by means of K-type thermocouples placed in the heating zone, 20 mm from the edge of the belt, 10 mm above the belt and at the centre of the MIR, as shown in Figure 7. The MIR intensity can be varied from 0 to 100%, with a maximum power supply of 3.7 kW for each of the emitters. The distance between the belt and the MIR lamps can be varied from 5.0 to 11.5 cm. Airflow is controlled by opening or closing the exit valve to the blower, and was measured by an anemometer.

The effect of pellet size was also tested during LaDePa processing experiments.



FIGURE 7. THERMOCOUPLE POSITION FOR TEMPERATURE MEASUREMENTS IN LABORATORY-SCALE LADEPA

The various tests are summarised in Table 2. In order to study the influence of each parameter, the parameter under investigation was varied while the other variables were kept constant. The reference conditions were: MIR intensity of 50%; MIR height of 11.5 cm; pellet diameter of 8 mm; fully-open air suction valve.

TABLE 2. SUMMARY OF CONDITIONS UNDER INVESTIGATION

Parameter to investigate	Range	Parameter of action	Range of operation
Temperature	80-220°C	MIR intensity	30 to 80%
		MIR height	6 to 11.5 cm
Residence time	4 to 40 min	Belt speed	0 to 100%
Pellet diameter	8 to 14 mm	Extruder outlet plate size	8 ,10, 12 and 14 mm
Air flowrate	4.6 to10.4 m <sup>3</sup> /min	Air flowrate valve	Fully open or closing the outlet valve

### 2.3.3 MEASUREMENT OF TEMPERATURE WITHIN THE PELLETS

The temperature within the pellets was measured during drying in LaDePa by the means of a thin K-type thermocouple introduced in the middle or near the surface of the pellets.

### 2.3.4 CHARACTERISATION OF THE FAECAL SLUDGE AND PROCESSED PELLETS

Pellets produced by the handheld extruder were placed on the belt and dried at various conditions. The processed pellets were collected and stored in zip lock bags for further analysis. Table 3 shows a summary of the various tests that were carried out on the faecal sludge and processed pellets, the required equipment and the methods used to prepare and analyse samples.

The moisture, volatile matter and ash content assist in characterising the drying process. The Ascaris egg content determines the pasteurisation efficiency. Ascaris are used as an indicator of pasteurisation as they are the most resistant pathogen to commonly applied pasteurisation methods. If Ascaris eggs have been deactivated, all other pathogens can be assumed to be destroyed too. The chemical analysis (phosphates, ammonia, nitrates, nitrites, phosphorus, potassium, calcium, magnesium, carbon, nitrogen, sulphur) provide information on the agricultural value of the processed pellets. Thermal conductivity, heat capacity, thermal diffusivity and calorific value provide the thermal characteristics of the pellets necessary to be used as a biofuel. The Ascaris content analysis was performed by external laboratories. The rest of the analysis was conducted internally in the laboratory of the Pollution Research Group located in the Chemical Engineering building at the University of KwaZulu-Natal (UKZN).

Rheological tests on the raw faecal sludge were also carried out. The main results are presented in **Appendix 1**.

**TABLE 3. ANALYSIS TO BE CARRIED OUT ON THE FAECAL SLUDGE AND PELLETS PROCESSED IN THE LABORATORY-SCALE LADEPA**

<b>Property</b>	<b>Analytical tests</b>	<b>Equipment/ Method</b>
<b>Proximate composition</b>	Moisture content	Oven dry 105°C
	Ash / volatile solid content	Furnace incineration at 550°C
<b>Biological</b>	Ascaris egg concentration	External laboratory
<b>Chemical</b>	Soluble phosphates, nitrites, ammonia, nitrates, nitrites	Blending of the sample with water + centrifugation + use of reactive kits with the liquid fraction + analysis in the Spectroquant, <i>Nova 60- Merck</i>
	Potassium, phosphorous, magnesium, calcium	Digestion of the solid + analysis in the MP-AES (Microwave Plasma – Atomic Emission Spectroscopy), <i>Agilent 4100</i>
	Carbon, Nitrogen	CN analyser, <i>LECO TrueMac</i>
<b>Thermal</b>	Thermal conductivity	Thermal conductivity analyser, C-therm TCI
	Heat capacity	Thermal conductivity analyser, C-therm TCI
	Thermal diffusivity	Thermal conductivity analyser, C-therm TCI
	Calorific value	Bomb calorimeter, <i>Parr 6200</i>

## 2.4 ERROR ANALYSIS

The error bar from the measurement was calculated by applying a Student’s t-distribution law in a confidence interval of 90% or 95%.

In the next Chapter, the results from experiments are discussed.

### 3. RESULTS AND DISCUSSION

In order to characterise the drying and pasteurisation of pellets in the LaDePa machine, various parameters were investigated. From the moisture content measured at different residence times, drying curves were plotted in order to evaluate drying kinetics, whilst volatile solids and ash content were determined in order to understand how the properties of the dried solid could change during the process. From the measurements of temperature at the core and surface of the pellets, the thermal history of the pellets through the treatment processes were obtained, which enables to a better understanding of the drying processes in our context. Through the calculation of the moisture removal as a function of the supplied power and the measurement of *Ascaris* eggs concentration, the drying and pasteurisation efficiencies of the process were evaluated. The chemical and thermal properties of the dried sludge, and their variability as a function of the operating conditions were determined in order to evaluate their potential use in agriculture or as a biofuel.

This chapter has four subsections that details the parameters affecting drying (**section 3.1**), the drying process (**section 3.2**), the efficiency of the LaDePa process (**section 3.3**) and the characterisation of the LaDePa product (pellets) (**section 3.4**).

#### 3.1 PARAMETERS AFFECTING DRYING PROCESS IN LADEPA

This section provides the results from drying experiments performed with the LaDePa laboratory prototype. Four variables that could affect the drying process were evaluated, including: drying temperature, MIR intensity, emitter height and airflow around the extruded pellet.

##### 3.1.1 DRYING TEMPERATURE

The temperature in the heating zone from the LaDePa machine can be adjusted through the MIR intensity and the emitter height with respect to the conveyer belt.

Table 4 shows the MIR intensity from each emitter to achieve a given temperature for the three cases tested in this work. Note that, to achieve the same temperature, each emitter has to be positioned at a different MIR intensity. The MIR intensity to refer to each of the cases in this work was the same than the intensity from the second emitter. The temperature, measured by a thermocouple, is only an indicator and it does not represent the real temperature on pellets.

**TABLE 4. CORRESPONDING MIR INTENSITIES AND TEMPERATURES**

MIR intensity %			Measured temperature (°C)
Reference	Emitter 1	Emitter 2	
30	25	30	87 ± 4
50	43	50	137 ± 4
80	72	80	215 ± 6

##### 3.1.1.1 EFFECT OF MIR INTENSITY AT CONSTANT EMITTER HEIGHT

The drying curves obtained at three different MIR intensities, at a constant emitter height of 11.5 cm, are shown in Figure 8. The effect of drying at different MIR intensities on the volatile matter and ash content of the pellets is shown in Figure 9.

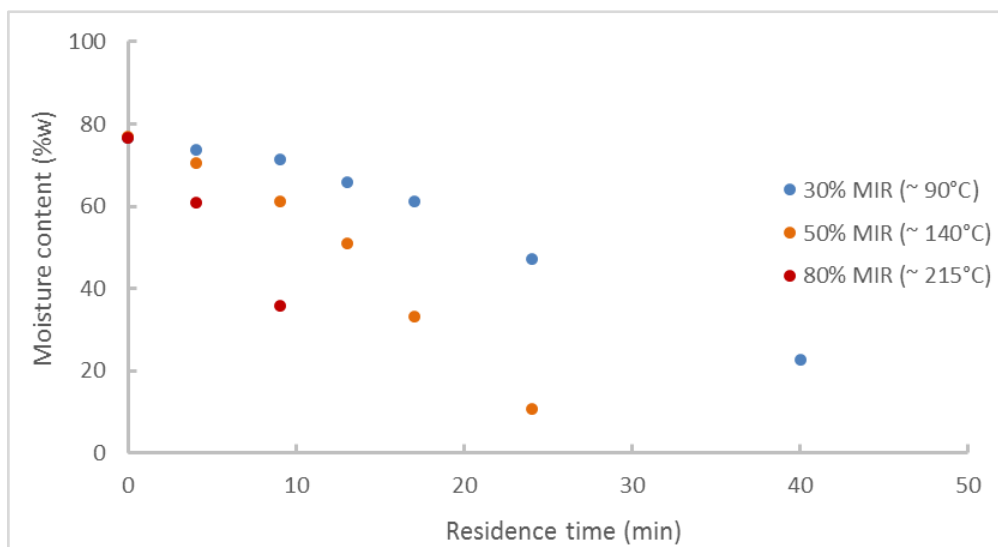


FIGURE 8. DRYING CURVES AT VARYING MIR INTENSITY, AT CONSTANT EMITTER HEIGHT (11.5 CM), FOR THE 8 MM PELLETS

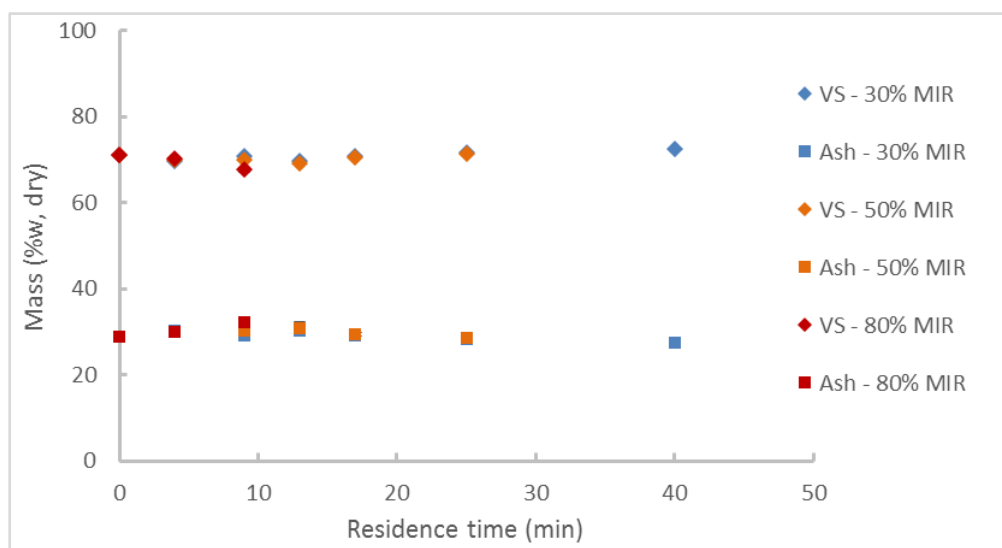


FIGURE 9. VOLATILE SOLIDS (VS) AND ASH CONTENT AT VARYING INTENSITY AND RESIDENCE TIME, AT CONSTANT EMITTER HEIGHT (11.5 CM), FOR THE 8 MM PELLETS

As expected, the increase of MIR intensity leads to faster drying. At 80% MIR intensity, the pellets were dried at the fastest rate but they were burned for residence times longer than 8 minutes. For that reason, no moisture content measurements could be performed after 8 minutes. The most optimal drying conditions were obtained for the intermediate MIR intensity (50%), by decreasing the moisture content up to 10% after 25 minutes of residence time without any thermal degradation of the sample. At the lowest MIR intensity (30%), the moisture content was decreased to 20% only after 40 minutes of residence time.

The volatile solids and ash content in the samples collected do not present any particular trend at varying MIR intensity. Most of the samples analysed had an ash content comprising between 0.28 and 0.32 g / g of dry solid, and a volatile solid content between 0.69 and 0.72 g / g of dry solid. The outlier

sample corresponds to that obtained at the highest heating intensity (80%), after 8 minutes of residence time, with a slightly lower volatile solid content and slightly higher ash content.

According to these results, the dried solid composition seems to not undergo considerable changes during drying, with the exception of the sample dried at the highest heating intensity after 8 minutes of residence time. In the latter case, the modification of the dried solid composition could be issued from a starting thermal degradation of the sample.

In summary, the optimal drying temperature is obtained at intermediate MIR intensities, where the drying rate is fast enough without risks of thermal degradation. At temperatures higher than 200°C, drying is the fastest but thermal degradation of the pellets is likely to occur. In the absence of any thermal degradation, the dried solid has no major physical modification.

### 3.1.1.2 EFFECT OF EMITTER HEIGHT AT CONSTANT TEMPERATURE

The height of the emitters with respect to the conveyer belt also have an influence on the drying rate. It is well known that the radiation intensity received by a body increases as the latter is closer to the radiative source. Figure 10 shows the behaviour of the drying curves by changing emitter height and adjusting the MIR intensity so that the temperature is maintained constant at 140°C.

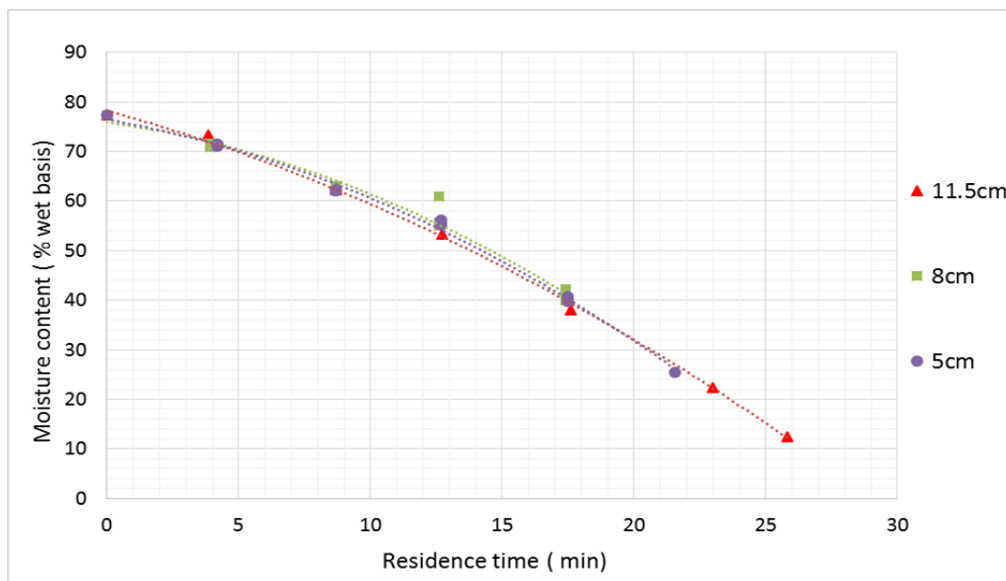


**FIGURE 10. DRYING CURVES AT VARYING HEIGHTS OF THE MIR EMITTER ABOVE THE BELT, AT CONSTANT TEMPERATURE (~ 140°C) AND MIR INTENSITY, FOR THE 8 MM PELLETS**

It can be seen that the same drying curve is obtained for the different cases. This means that drying occurs similarly for different combinations of MIR intensity and emitter height on condition that the solid is exposed to the same temperature. This result has important implications on the process. It is preferable to operate at a short distance between the conveyer belt and the emitters, than a large one which will require a higher MIR intensity to achieve the same results.

Operating at the shortest possible distance between the MIR emitters and the conveyer belt will lead to energy consumptions savings, which will be reflected in lower operating costs of the installation.

### 3.1.2 AIRFLOW AROUND THE PELLET

In the LaDePa process, the hot exhaust air from the diesel engine is introduced into the drying chamber in order to remove the evaporated moisture from the solid surface and provide supplementary heat for evaporation. In the laboratory prototype, there is also circulation of air in the heating zone, but in this case, the stream is air from the environment and thus it is at ambient temperature. Therefore, in the laboratory-scale LaDePa, the air stream in the heating zone is beneficial in terms of mass transfer of evaporated moisture, but negative from a thermal perspective, as the pellets could be potentially cooled. Two experimental cases were studied in order to determine the effect of the airflow rate on drying: by varying the flow rate at constant drying temperature and at constant MIR intensity.

#### 3.1.2.1 EFFECT OF AIRFLOW RATE AT CONSTANT MIR INTENSITY

During the first set of experiments, the airflow rate was varied at constant MIR intensity for the 8 mm pellets. Figure 11 shows the resulting drying curves for the airflow rate obtained with fully-open valve ( $6.3 \text{ m}^3/\text{min}$ ) and half open valve ( $10.4 \text{ m}^3/\text{min}$ ).

No difference could be observed from the drying curves obtained at the different air flowrates. A possible explanation to this is that the increase of air flowrate enhances mass transfer phenomena but leads to a cooling of the pellets. In the end, both opposing effects counterbalance one another and thus the drying rate remains approximately the same.

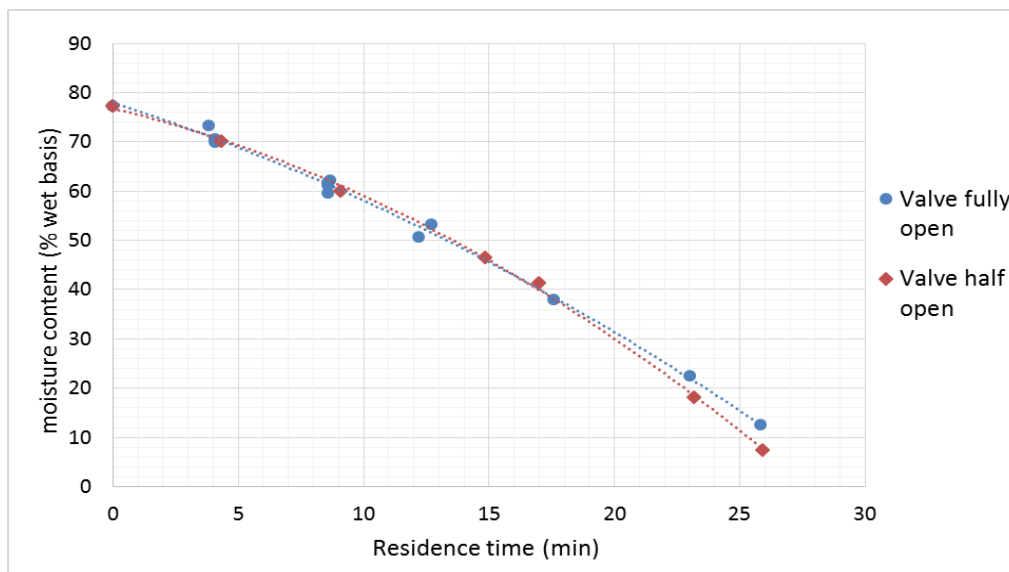
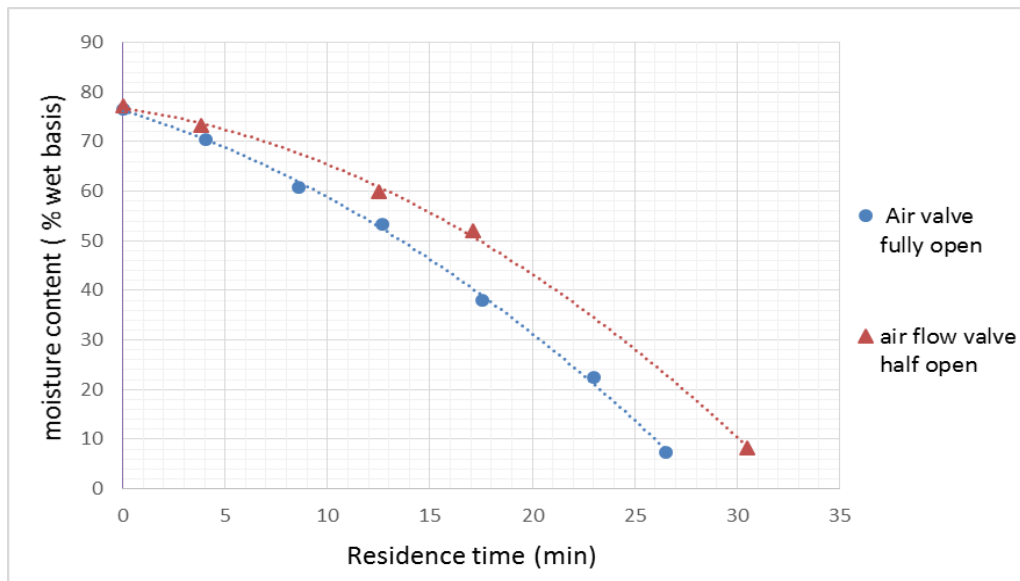


FIGURE 11. DRYING CURVES FOR DIFFERENT AIRFLOW RATES AT CONSTANT MIR INTENSITY (50%), FOR THE 8 MM PELLETS

#### 3.1.2.2 EFFECT OF AIRFLOW RATE AT CONSTANT DRYING TEMPERATURE

In order to highlight the effect of the air flowrate on mass transfer only, experiments at constant temperature were carried out. As the air flowrate was increased from  $6.3$  to  $10.4 \text{ m}^3/\text{min}$ , corresponding to the half and fully open valve respectively, the MIR intensity was increased in order to offset the increased cooling effect of air to maintain a constant temperature of  $140^\circ\text{C}$ . The drying curves obtained from this set of experiments are depicted in Figure 12.



**FIGURE 12. DRYING CURVES FOR DIFFERENT AIRFLOW RATE AT CONSTANT DRYING TEMPERATURE ( $\sim 140^{\circ}\text{C}$ ), FOR THE 8 MM PELLETS**

The drying rate is faster when the valve is fully open rather than half open, which shows the positive effect of increasing air flowrate on drying in terms of mass transfer.

The increase of air flowrate in the drying zone has a positive effect on the drying rate, as it enhances the mass transfer of the evaporated moisture from the surface of the solid to the surroundings. However, this effect can be decreased if the gas introduced is not heated, as the surface of the solid could then be cooled affecting the drying rate.

### 3.1.3 EFFECT OF THE PELLET SIZE

The effect of the pellet size on drying was also investigated at constant MIR intensity (50%) and emitters height (11.5 cm). The drying curves obtained for the 8, 10, 12 and 14 mm diameter pellets are plotted in Figure 13.

As it could be expected, pellets with larger diameter take longer time to dry compared to those with smaller size. So, the 14 mm diameter pellet has the lowest drying rate while the 8 mm pellet has the highest one. At a residence time of 26 min, pellets with a diameter of 8 mm are dried to below 10% moisture content while those with a diameter of 14 mm have a moisture content of 53%. The 10 mm and 12 mm pellets have intermediate drying rates.

The pellet diameter is an important parameter for the drying process. In order to achieve faster drying rates, it is very important to reduce the pellet size as much as possible.

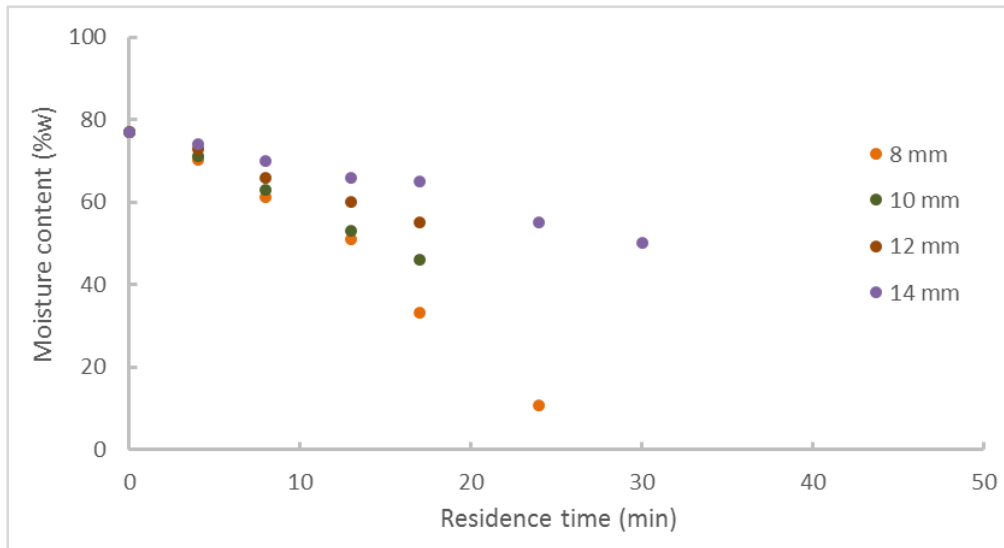


FIGURE 13. DRYING CURVES FOR DIFFERENT PELLET DIAMETERS

### 3.1.4 BULKING PRE-TREATMENT OF SAMPLE

In Figure 14, the drying curve from the raw faecal sludge is compared to that obtained by adding sawdust to the sample and by pre-drying it. The drying curves were normalised with respect to the initial moisture content, so that the curves start at the same point. The moisture content of the faecal sludge with and without sawdust was close to 80%. The moisture content of the pre-dried sample was decreased approximately to 70%.

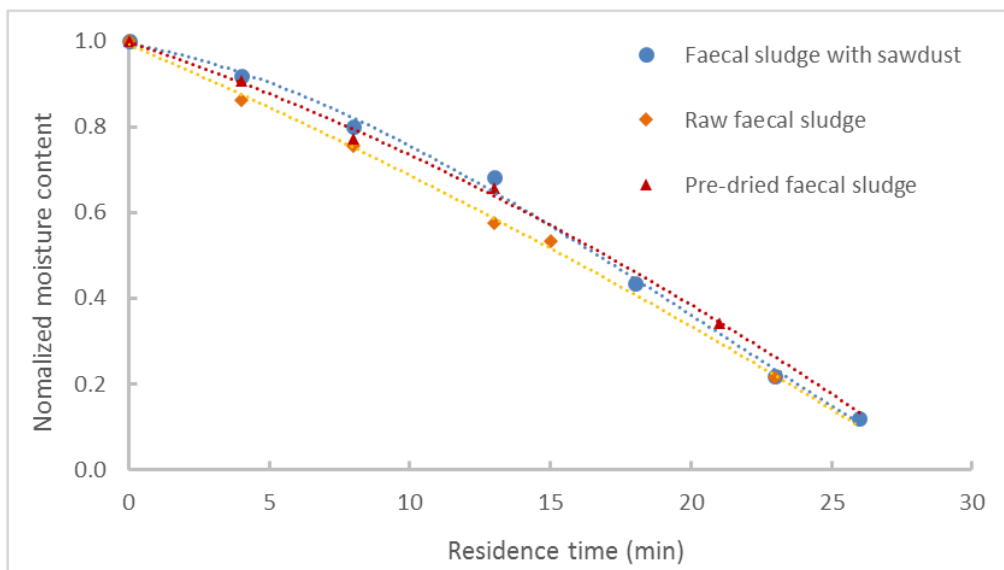


FIGURE 14. DRYING CURVES FOR DIFFERENT SAMPLES, FOR THE 8 MM PELLETS

Note that faecal sludge with sawdust was the most widely used sample in this work, as the addition of sawdust facilitates pellet formation (refer to **section 2.3.1** Extrusion).

During most of the transformation, the drying of raw faecal sludge was slightly faster than the other cases. The drying of the faecal sludge with sawdust and the pre-dried sample progressed at a similar rate. At the end of the transformation, the three drying curves converged.

Pre-drying and addition of sawdust slightly lowers faecal sludge drying rate. In the case of pre-dried faecal sludge, this result could be explained as the most easily removable moisture has already been taken out, and the remaining moisture is more difficult to remove.

## 3.2 DRYING PROCESS

This section presents the results from the drying experiments.

### 3.2.1 TEMPERATURE WITHIN THE PELLETS DURING DRYING

Temperature measurements were performed at the core and near the surface (on the top and on the lateral side) of the 8 mm and 14 mm pellets during experiments in the laboratory-scale LaDePa prototype. Figure 15 displays the temperature measured as a function of the distance conveyed in the machine.

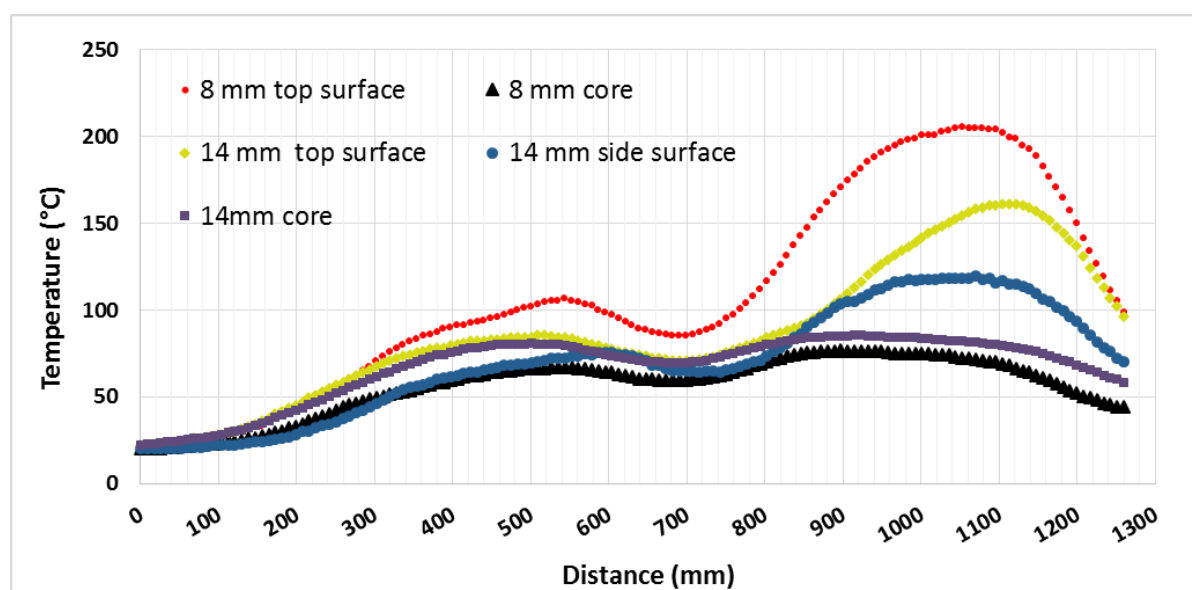


FIGURE 15. TEMPERATURE MEASURED IN THE 8 AND 14 MM PELLETS VERSUS THE DISTANCE CONVEYED, DURING EXPERIMENTS AT 50% MIR INTENSITY AND RESIDENCE TIME AROUND 20-25 MINUTES

For each case, the temperature increases until reaching a plateau value, then decreases in temperature before increasing again until reaching a second plateau, and then finally decreases. Each temperature increase should correspond to the passage of the pellets under one of the MIR emitters. The decrease of temperature should happen after the pellets have left the zone exposed to the MIR radiation.

The thermal history is similar between the 8 and 14 mm pellets at the core, with temperatures ranging between 60 and 80°C. At the near surface of the pellets, the temperature reaches a higher temperature than at the core during the process and depends on the sample size. Under the first MIR emitter, the temperature difference between the core and the surface is low for the 8 mm pellets or null for the 14 mm pellets. Under the second emitter, this difference drastically increases: the top surface of the solid attains a temperature of 200°C for the 8 mm pellets and 160°C for the 14 mm pellets, while at the core the temperature remains around 70-80°C. In the case of the 14 mm pellets, the temperature on the lateral surface, not exposed to the IR radiation, is lower than at the top side, directly positioned under the IR radiation.

Under the first MIR emitter, the 14 mm pellets can be considered as isothermal. This is not the case of the 8 mm pellets where the surface gets a slightly higher temperature than the core. Under the second emitter, the temperature at the surface drastically increases but the temperature at the core remains almost unchanged, for both the 8 and 14 mm pellets. It is well known that the temperature of a wet material being dried is determined by the temperature of moisture evaporation. This could explain that the temperature at the core of the solid and at the surface at the beginning of the process remains quite constant in the range 60-80°C. After a certain processing time, the surface of the pellets is dried and subsequently its' temperature increases while the wet core remains at the moisture evaporation temperature. The size of the pellets has an important influence on this process: the surface is dried first and the dried surface attains a higher temperature for the 8 mm pellets compared to the 14 mm pellets, possibly as the heating flux is higher as the solid has a smaller size. The MIR radiation from the emitters is received on the top surface of the pellets, which is, in consequence, at a higher temperature compared to the rest of the surface.

Note that the temperature reached at the surface of the 8 mm pellets is considerable higher than that measured by the thermocouple for this series of experiments (~ 150°C). As previously indicated (**section 3.1.1 Drying temperature**), the temperature measured from the thermocouple is only an indicator and can differ from the real temperature on the pellets. Accordingly, during experiments at 80% MIR intensity, the temperature on the 8 mm pellets should attain considerable higher temperatures than that indicated by the thermocouple, 215°C, which explains the thermal degradation suffered by the pellets under these severe conditions.

During the LaDePa process, the heat from the MIR irradiated by the emitters is received by the pellets at the top surface and then conducted to the rest of the surface and inside the solid. At the initial stage of drying, the pellets are isothermal, when the overall state of the solid is wet. As the near surface is dried, the temperature in this zone increases, while the wet core remains at the moisture evaporation temperature. The higher heating flux received for the pellets of smaller size leads to a sooner and more drastic increase of surface temperature compared to larger pellets. If the MIR radiation intensity is too high, the dried surface of the pellet could reach high enough temperatures to suffer from thermal degradation and burning in the worst case. In this case, the top of the pellet will be the first affected zone.

### 3.2.2 KINETIC STUDY OF PELLETS DRYING

The drying kinetics during LaDePa experiments were studied by plotting the moisture content on a dry basis versus the residence time. Figure 16 presents the plots obtained at different MIR intensities and pellet diameters. The moisture content on dry basis is referred to as the ratio of the mass of moisture with respect to the mass of dry solid.

In Figure 16A and B, it can be seen that, for the different cases, the moisture content decreases linearly until reaching a value between 1.5 and 2.0 g / kg dry solid. After this point, the moisture removal continuously slows down with the progress of time.

According to drying theory, the linear decrease described above corresponds to the constant rate period. During this stage, drying of the solid takes place at the surface, which is supposed to be saturated in moisture. As a consequence, the drying kinetics are mostly controlled by the external factors. The decrease of the drying rate after the linear section is known as the *falling rate* period,

which occurs after that the solid surface becomes unsaturated in moisture or completely dried. At this stage, the moisture diffusion within the solid to the surface has a considerable influence on drying kinetics.

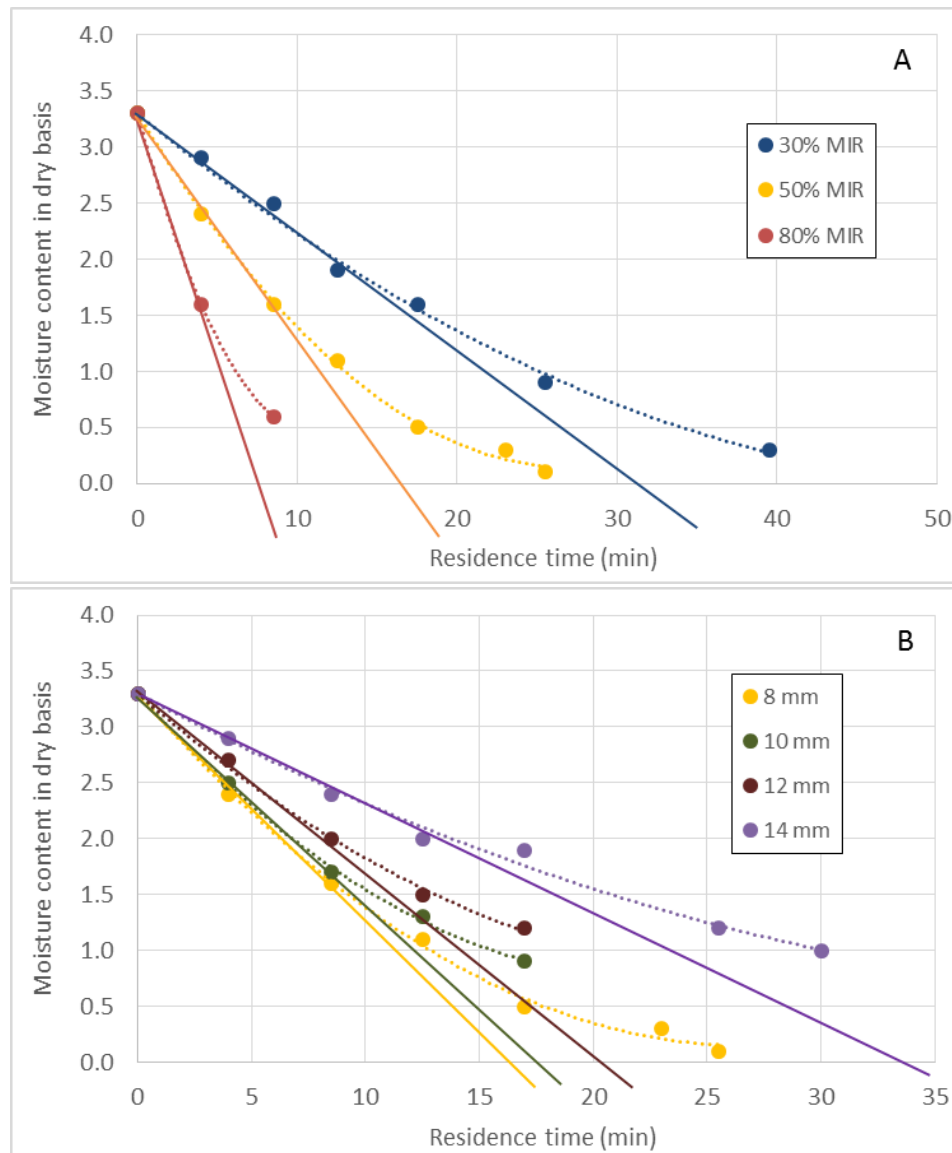


**FIGURE 16. MOISTURE CONTENT IN DRY BASIS VERSUS RESIDENCE TIME AT DIFFERENT MIR INTENSITIES FOR THE 8 MM PELLETS (A) AND FOR DIFFERENT PELLET DIAMETERS AT 50% OF MIR INTENSITY (B)**

The transition between the two kinetic regimes occurs at the critical moisture content. In the present study, the critical moisture content varies between 1.5 and 2.0 g / kg on a dry basis (Figure 16), which corresponds to 60 to 65% in wet basis. It can be noticed that the critical moisture content tends to decrease as the drying rate is faster.

During drying, the removal of approximately half of the moisture occurs at the constant rate period. Theoretically, the surface of the pellets should remain completely wet during this period. Thereafter, the falling rate period follows, indicating that the pellet surface is possibly fully or partially dried. At this stage, the temperature on the pellet surface can increase until causing thermal degradations, if the heating intensity is enough high.

### 3.3 EFFICIENCY OF THE PROCESS

This section has two sub-sections which focus on the drying (**section 3.3.1**) and pasteurisation (**section 3.3.2**) efficiency, respectively.

#### 3.3.1 DRYING EFFICIENCY

During operation in the laboratory-scale LaDePa, most of the power is consumed by the MIR emitters. A minor part of the power is used for mechanical work, operation of the control panel and temperature measurements. The correlation between the MIR intensity and the consumed power by the two emitters is given in Table 5.

TABLE 5. CORRELATION BETWEEN THE MIR INTENSITY AND THE POWER CONSUMED

MIR intensity %	Power (kW)
30	3.0
50	4.7
80	6.5

Based on the power consumed by the MIR emitters and the drying curves presented in **section 3.1** **PARAMETERS AFFECTING DRYING PROCESS IN LADEPA**, the drying efficiency, here expressed as the moisture removal as a function of the energy consumed, was estimated for different experimental cases.

##### 3.3.1.1 DRYING EFFICIENCY AS A FUNCTION OF MIR INTENSITY

Figure 17 shows the moisture removed as a function of the power consumed for three different MIR intensities, at fixed emitter height (11.5 cm).

It can be seen that less energy is consumed to remove moisture as the MIR intensity is higher.

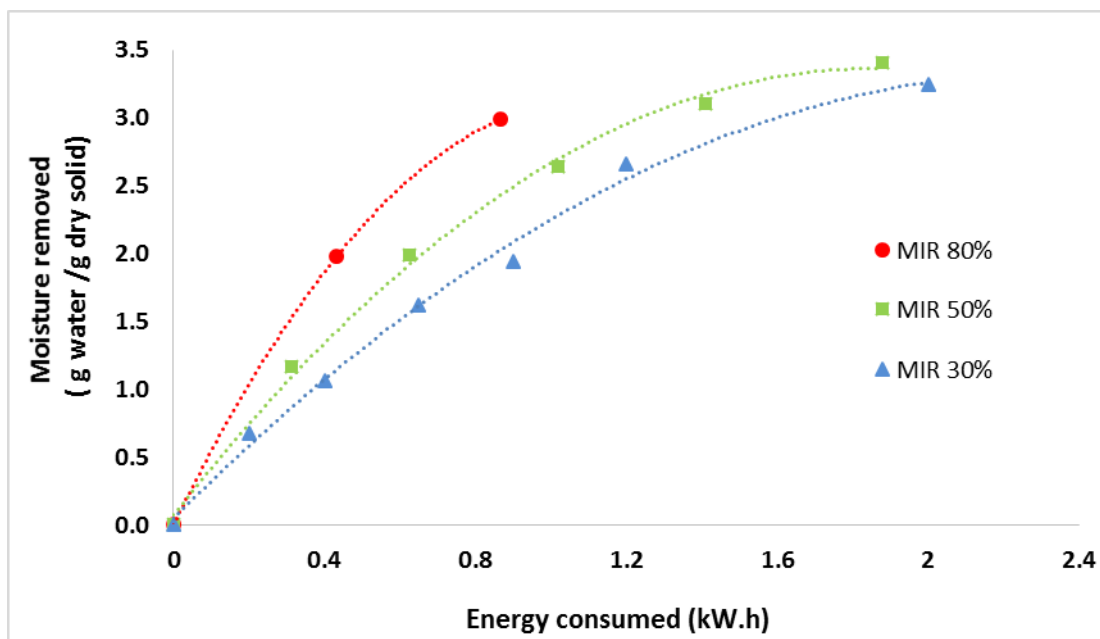


FIGURE 17. MOISTURE REMOVAL VERSUS ENERGY CONSUMPTION FOR DIFFERENT MIR INTENSITIES, AT FIXED EMITTER HEIGHT (11.5 CM), FOR THE 8 MM PELLETS

### 3.3.1.2 DRYING EFFICIENCY AS A FUNCTION OF MIR HEIGHT AT FIXED DRYING TEMPERATURE

Figure 18 shows the moisture removed versus energy consumed for different emitters heights above the belt, at fixed drying temperature ( $\sim 140^{\circ}\text{C}$ ) which was achieved by adjusting the MIR intensity. Indeed, if the distance between the emitters and the belt is reduced, the MIR intensity was decreased so that the same temperature is maintained.

It can be observed that the energy consumption decreases slightly by reducing the distance between the MIR emitters and the belt between 5 and 11.5 cm emitter height. This trend is less obvious for 8 cm. The conclusion from the experiments in this section indicate that operating at a lower distance between the emitter and the belt leads to the reduction of the energy consumed to remove moisture.

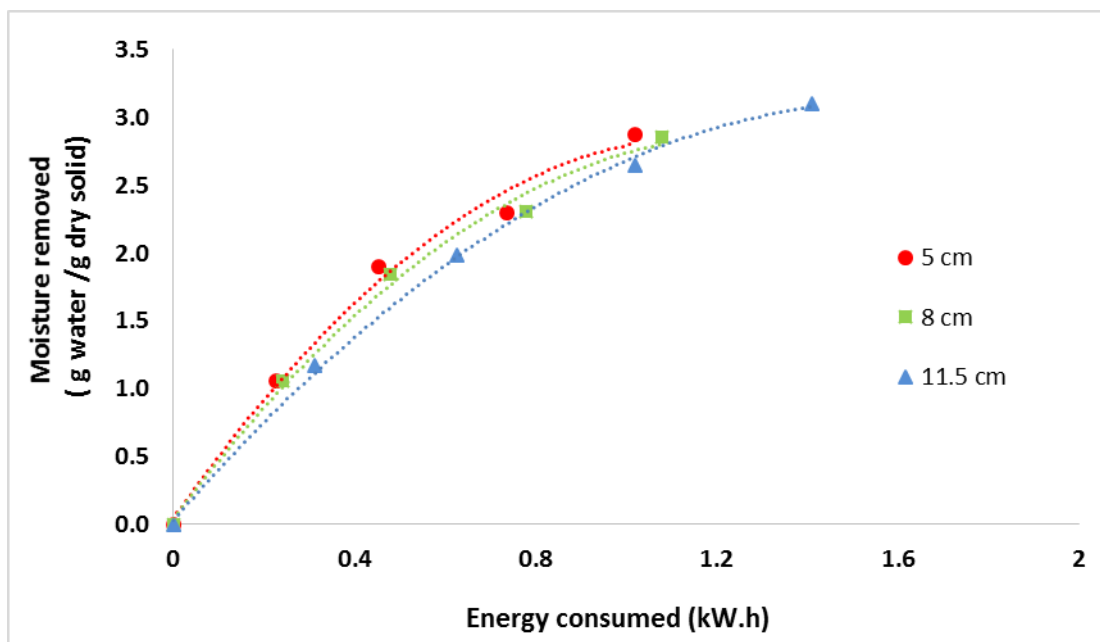


FIGURE 18. MOISTURE REMOVAL VERSUS ENERGY CONSUMPTION FOR DIFFERENT EMITTERS HEIGHTS, AT FIXED TEMPERATURE ( $\sim 140^{\circ}\text{C}$ ) AND VARIABLE MIR INTENSITIES, FOR THE 8 MM PELLETS

If the emitter height was varied at fixed MIR intensity, the differences from the trend described in the last paragraph would be enlarged. Indeed, if the MIR intensity was kept at 50% for the 8 and 5 cm emitters height instead to be reduced to maintain a fixed temperature, the power consumption to attain any moisture removal would be lower than that displayed in Figure 18.

### 3.3.1.3 DRYING EFFICIENCY AS A FUNCTION OF THE AIR FLOW RATE

The effect of the opening degree of the suction air valve on the power consumed to remove moisture is presented in Figure 19. The two different cases studied in the sections **3.3.1.1 Drying efficiency as a function of MIR intensity** and **3.3.1.1 Drying efficiency as a function of MIR intensity** are included in the same graph, i.e. half opening of the valve by maintaining the same MIR intensity and by adjusting the MIR intensity in order to maintain the same drying temperature than after fully opening the valve.

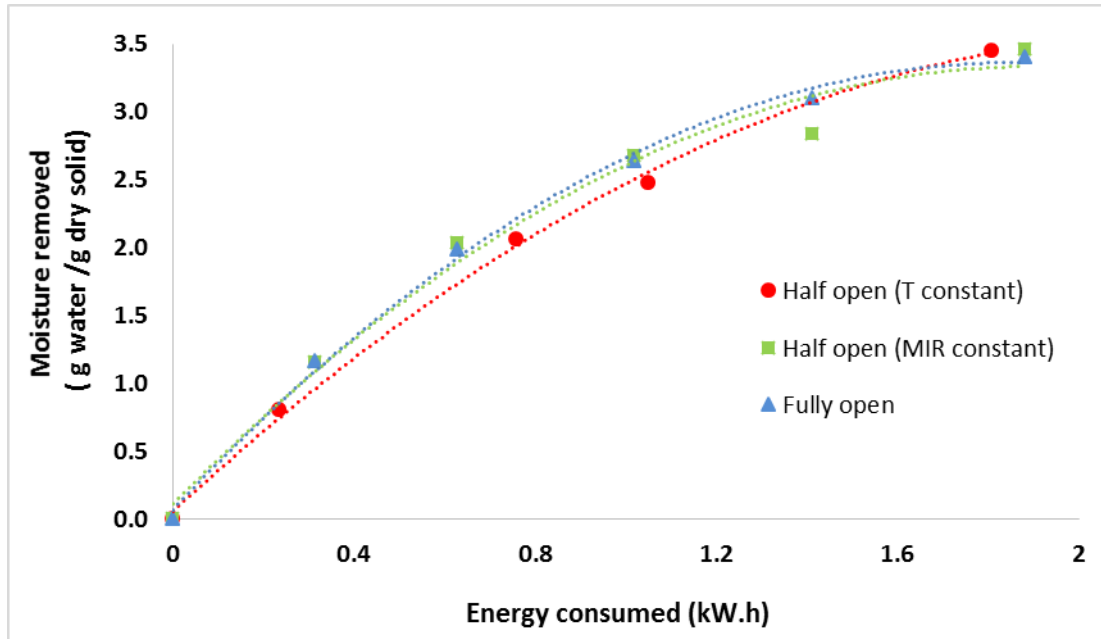


FIGURE 19. MOISTURE REMOVAL VERSUS ENERGY CONSUMPTION AS A FUNCTION OF THE AIR FLOWRATE (RELATED TO THE SUCTION VALVE OPENING DEGREE), FOR THE 8 MM PELLETS

The energy consumed to remove moisture is the same or close for the fully open valve, and the two cases of half open valve. Therefore, air flow rate is not an influent parameter on energy consumption for drying in our case. As discussed in the **section 3.1.2 Airflow around the pellet**, the beneficial effect of air flowrate increase in terms of mass transfer is counterbalanced by its increasingly cooling effect on the pellets, leading to a neutral global effect of the airflow rate. If the air was pre-heated as in the full-scale LaDePa, the cooling effect would not occur. By consequence, the energy consumption relative to moisture removal could be reduced, depending on the heating source used for air pre-heating.

## 3.3.1.4 DRYING EFFICIENCY AS A FUNCTION OF PELLET SIZE

Figure 20 displays the energy consumed for moisture removal in pellets of different diameters.

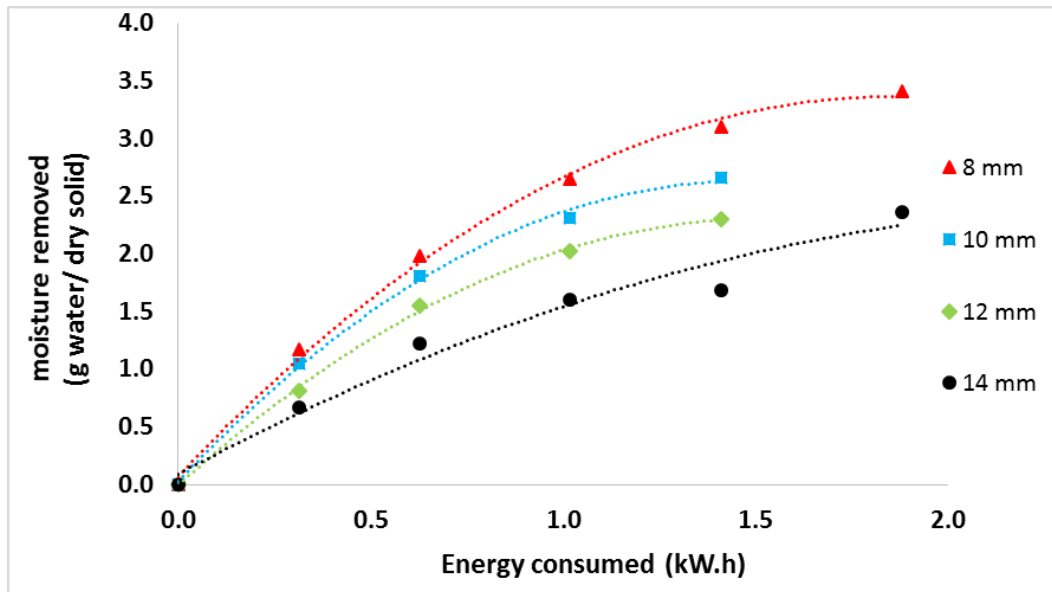


FIGURE 20. MOISTURE REMOVED VERSUS ENERGY CONSUMPTION FOR PELLETS OF DIFFERENT SIZES

More energy is consumed to remove moisture as the size of the pellets is increased. This result was expected as the heating of larger particles require more energy than that of smaller ones.

## 3.3.1.5 SUMMARY

Critical parameters on drying efficiency are the MIR intensity, the emitters height and the pellet size. In order to lead to a more efficient drying, energy savings can be achieved by increasing the MIR intensity, by reducing the distance between the emitters and the belt, and by decreasing the pellet size. However, the heating intensity received by the pellet should not exceed the limit from where the solid would be thermally degraded.

Under the explored conditions, the airflow rate is not a crucial parameter on drying efficiency. If the air was pre-heated by a low power consumption heating source (for instance by heat recovery from the process, by a renewable energy source or by a highly efficient electrical heater), the energy consumed for moisture removal could be decreased.

## 3.3.2 PASTEURISATION EFFICIENCY

Ascaris analysis was performed for the 8 and 14 mm pellets processed at different residence times and MIR intensities. Table 6 presents the concentration of Ascaris eggs, which are viable to develop and which are dead, in the raw sample and processed pellets. Note that the concentration of death Ascaris eggs was too high in the different samples to get any information about the pasteurisation effect of the process. The concentration of viable Ascaris eggs was the indicator which could be used for that purpose.

TABLE 6. ASCARIS EGG CONCENTRATION FOR VARIOUS SAMPLES PROCESSED AT DIFFERENT CONDITIONS

Sample	MIR intensity %	Residence time (s)	Ascaris eggs / g total solid	
			Viable	Dead
Faecal sludge	N.A.	N.A.	135	4144
Pellets 8 mm	30	8	13 (?)	5810
		17	0	5747
		25	0	6535
	50	8	3 (?)	6060
		17	0	6163
		25	0	4429
	80	4	0	6410
		8	0	4606
	Pellets 14 mm	50	8	0
17			0	5748
25			0	5212

The concentration of the viable *Ascaris* eggs in the raw faecal sludge is quite high, while most of the processed pellets does not present any viable eggs. A few viable eggs were detected for the 8 mm pellets processed at MIR intensity of 30% and 50% after 8 minutes of residence time. However, the aspect of these eggs was uncommon and looks like intermediary between viable and death eggs. So, they may have just recently died and not yet become "dead-looking".

From the concentration of the viable eggs, it can be deduced that 8 minutes of processing in the laboratory-scale LaDePa, for any of the pellet size, is enough for the *Ascaris* egg destruction or high damage leading to a posterior death. It also could be observed that *Ascaris* eggs complete deactivation could be achieved after 4 minutes of residence time for the 8 mm pellets under a MIR intensity of 80%. No measurements have been yet performed at 4 minutes of residence time for the other cases. Complete pasteurisation in LaDePa machine is ensured for residence times longer than 8 minutes.

### 3.4 CHARACTERISATION OF PELLETS

This section has two sub-sections which focus on the chemical (**section 3.4.1**) and thermal (**section 3.4.2**) analysis of LaDePa processed pellets, respectively.

#### 3.4.1 CHEMICAL ANALYSIS

The concentrations of the chemical key components for the use of the dried pellets in agriculture were determined. An elemental analysis was performed in order to measure the concentration of macronutrients, phosphorous (P) and potassium (K), and micronutrients, calcium (Ca) and magnesium (Mg). The concentrations of molecular compounds, such as phosphates ( $\text{PO}_4^{3-}$ ), nitrates ( $\text{NO}_3^-$ ), nitrites ( $\text{NO}_2^-$ ) and ammonia ( $\text{NH}_4^+$ ), were also measured.

##### 3.4.1.1 ELEMENTAL ANALYSIS

The concentrations on dry basis of C, N, P, K, Mg and Ca from the 8 mm pellets, processed at different residence times and MIR intensities, are shown in Figure 21, Figure 22 and Figure 23. It was verified

that the pellet size and air flowrate do not influence the chemical composition of the sample for some of the elements in **Appendix 4**.

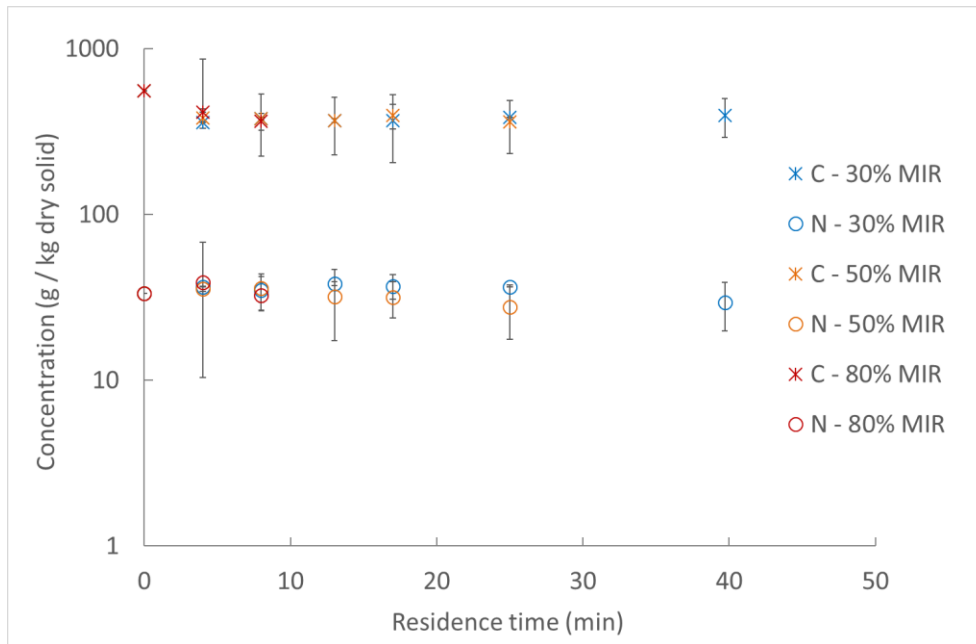


**FIGURE 21. CONCENTRATION OF C AND N IN THE 8 MM PELLETS PROCESSED AT DIFFERENT RESIDENCE TIMES AND MIR INTENSITIES**

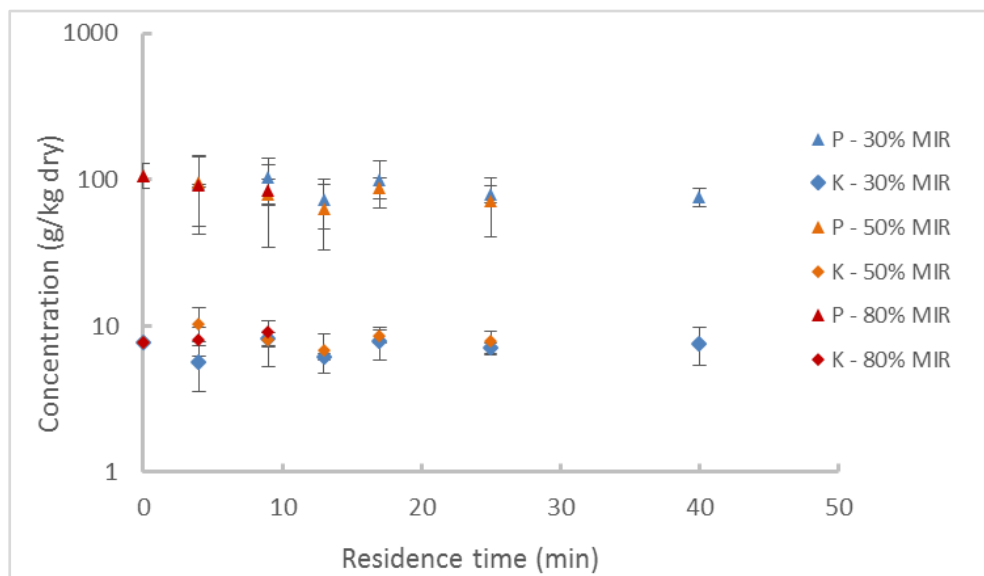


**FIGURE 22. CONCENTRATION OF P AND K IN THE 8 MM PELLETS PROCESSED AT DIFFERENT RESIDENCE TIMES AND MIR INTENSITIES**

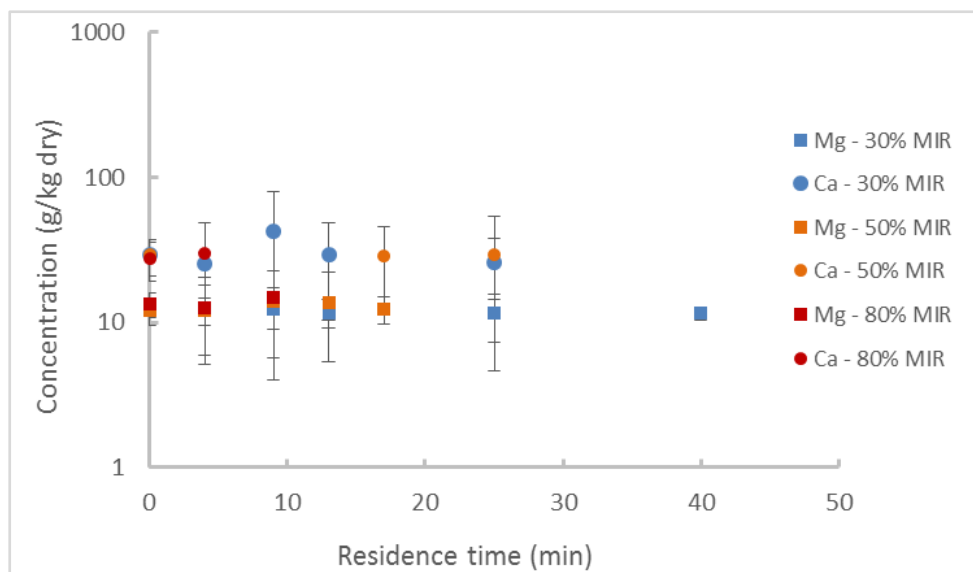


**FIGURE 23. CONCENTRATION OF MG AND CA IN THE 8 MM PELLETS PROCESSED AT DIFFERENT RESIDENCE TIMES AND MIR INTENSITIES**

It can be seen that the concentrations do not significantly change as a function of the operating conditions, which mean that drying does not affect the C, N, P, K, Mg and Ca concentrations in the pellets. The mean values for the C, N, P, K, Mg and Ca concentrations are 380, 35, 85, 10, 15 and 30 g / kg of dry solid respectively. As expected, C was the major constituent of faecal sludge, among the analysed elements.

The P concentration in the pellets is relatively high: it is higher than the typical P concentration from manures and home compost, which vary from 0.5 to 25 g / kg of dry solid [7, 12-14]; it is in the range of some typical industrial fertilisers as the ammonium phosphate sulphate (85 to 170 g / kg), slag basic (50 to 80 g / kg), superphosphate single (70 to 90 g / kg) and urea ammonium phosphate (55 to 180 g / kg) [15].

The K and N concentration in the pellets is lower than that from the usual industrial fertilisers [15], but it is in the range of that is usually found in manures and home composts (5 to 25 g / kg of dry solid; 5 to 50 g / kg of dry solid for N).

The concentration of the micronutrients are in comparable proportions to those from the macronutrients: the concentration of Mg is similar than that K; the concentration of Ca is about three times higher than that K, and three times lower than that P. The micronutrient content of the dried pellets is in the range of typical manure and compost (5 to 10 g / kg dry solid for Mg; 30 to 90 g / kg dry solid for Ca) [7, 12, 14].

#### 3.4.1.2 MOLECULAR COMPOUNDS

The concentrations of the nutrients in their different molecular form are very important to determine, as the plants assimilate more easily some molecules than others. For example, nitrogen is preferentially taken up by plants as nitrates rather than ammonia or nitrites. According to the experimental method conducted for these measurements (**section 2.4**), only the water-soluble

fraction of the compounds can be measured. The fraction of the compounds linked to the solid matrix is not accessible. Nonetheless, the soluble fraction of the compounds is an important indicator for the use of pellets in agriculture, as it would be quickly released in the soil (for example after a rainfall) and then be accessible the first to the plants.

Because of the high dispersion of the results obtained in the Merck Spectroquant, it was not possible to get precise data. Only rough estimations of the soluble compounds concentration in the early and advanced drying stage could be determined. The order of magnitude of the soluble compound concentrations is displayed in Table 7.

**TABLE 7. ORDER OF MAGNITUDE OF THE CONCENTRATION OF AMMONIA, NITRATES, NITRITES AND PHOSPHATES IN THE 8 MM PELLETS DURING DRYING**

Compound	Concentration (g/ kg dry solid)	
	Early drying stage (moisture content > 70%)	Advanced drying stage (moisture content < 40%)
$\text{NH}_4^+$	~ 30	~ 10
$\text{NO}_3^-$	~ 1	~ 0.1
$\text{NO}_2^-$	~ 10	~ 1
$\text{PO}_4^{3-}$	~ 10	~ 10

Among the nitrogenous compounds, ammonium was the major compound, followed by nitrites and finally nitrates, which were found in very small amounts. In the raw sludge, the sum of the ammonium, nitrates and nitrites concentration was roughly 40 g/kg dry solid, equivalent to a nitrogen content of approximately 25 g/kg dry solid, which is close to the measured total nitrogen content (32 g/kg dry solid). This result suggests that the nitrogen in faecal sludge is mostly found as ammonium, nitrates and nitrites. Nonetheless, the concentration of these compounds decreased as moisture was removed during drying. In the dried pellets, the nitrogenous compounds concentration dropped to roughly 10 g/kg dry solid, whereas the total nitrogen content remained constant during drying, as observed in **section 3.4.1.1**. The decrease of the ammonium, nitrates and nitrites concentration could be a result of chemical changes during drying, in particular bonding of compounds with the dry bone structure.

The soluble phosphate concentration remains constant during drying, at roughly 10 g/kg dry solid. The soluble phosphorous content is then around 3 g/kg dry solid, which represents 4% of the total phosphorous (**section 3.3.1.1**). The fraction of soluble phosphate is then considerably lower compared to the total phosphorous.

#### 3.4.1.3 SUMMARY

The pellets obtained from LaDePa contains high amounts of carbon with a rich inorganic nutrient composition, which makes it suitable to use it in agriculture as organic fertilizer or soil conditioner. It presents a relative high phosphorous content which is comparable to some industrial fertilisers and is higher than usual manure and home composts. Moreover, its potassium, calcium and magnesium contents, which are comprised in the range from manure and home composts common composition, are acceptable.

Drying does not affect the composition of the nutrient elements, even in the case of nitrogen where a loss as volatilization in the form of ammonia could be expected. However, it was observed that drying affects the chemical form of nitrogen in the sludge. In the raw material, nitrogen is found mainly as ammonium, nitrates and nitrites that can be drawn off from sludge through leaching relatively easily. In the dried material, nitrogen becomes difficult to remove as it may be bonded to the solid structure. As an implication of this, it can be supposed that the dried sludge will slowly release the nitrogen if used for agricultural purposes. This will contrast with the use of raw sludge in agriculture where the release of nitrogen could be considerably faster, for example after irrigation or a rainfall. Therefore, the availability of the fast release nitrogenous compounds decreases as drying proceeds.

Concerning phosphorous, only a small fraction is in the form of phosphates that can be removed. Hence, most of the phosphorus, probably strongly bonded in the solid matrix, could be assumed to be slowly released in the soil. Only a small fraction of phosphorous will be quickly released as phosphates in the soil. No apparent chemical modification of phosphorus was detected during drying.

### 3.4.2 THERMAL ANALYSIS

Thermal analysis was performed on the LaDePa pellets in order to evaluate its potential as biofuel. The properties measured were the calorific value, thermal conductivity, heat capacity and thermal diffusivity.

#### 3.4.2.1 CALORIFIC VALUE

Figure 24 shows the calorific value measured for the 8 mm pellets, processed at different MIR intensities and after different residence times. In **Appendix 4**, it was verified that the pellet size does not have an influence on calorific value.

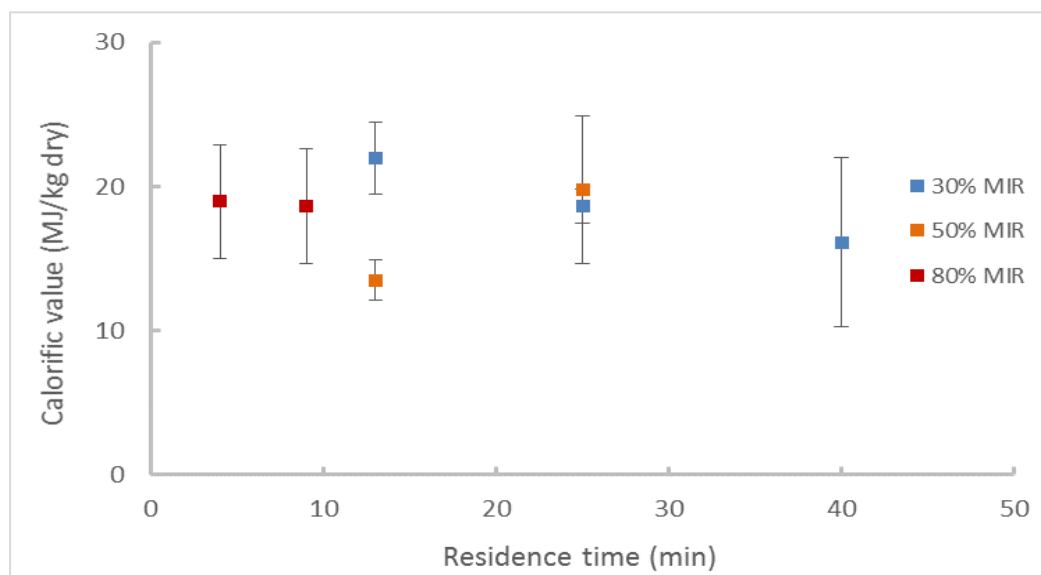


FIGURE 24. CALORIFIC VALUE FOR THE 8 MM PELLETS AT DIFFERENT RESIDENCE TIMES AND MIR INTENSITIES

The calorific value for the pellets obtained at different conditions is very similar: 18 MJ/kg dry solid. This means that the calorific value of the material is not affected during processing in LaDePa.

The value of the calorific value from the pellets is quite high: it is similar to the calorific value from wood and some coal ranks as lignite, bituminous coal and peat (14-25 MJ/kg) [16]; it represents around half or one third of the calorific value of diesel, natural gas and coal ranks as anthracite (30-45 MJ/kg) [16].

### 3.4.2.2 THERMAL CONDUCTIVITY

Figure 25 presents the calorific value measured for the 8 mm pellets, obtained after processing in the LaDePa at different MIR intensities and different residence times.

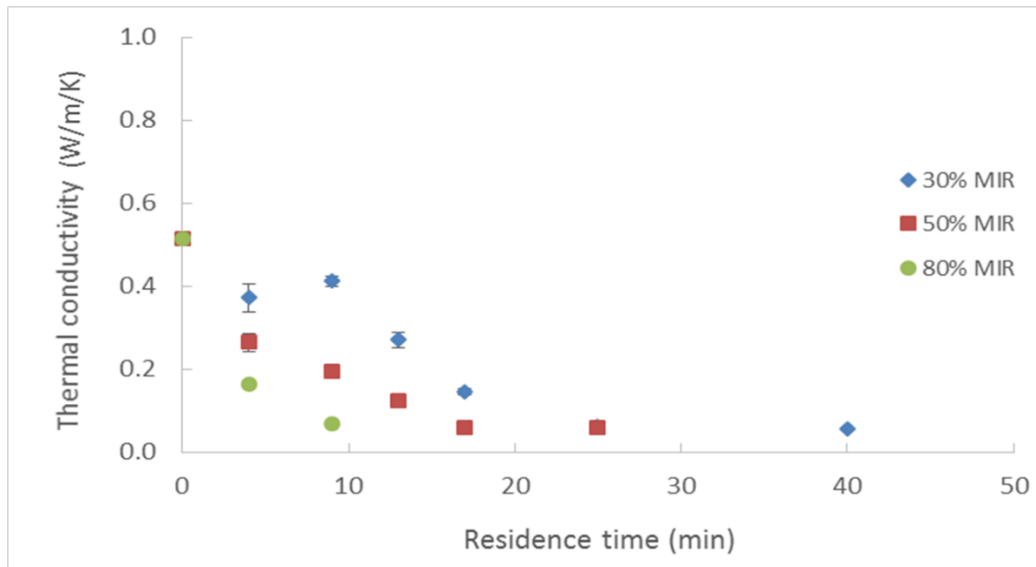


FIGURE 25. THERMAL CONDUCTIVITY FOR THE 8 MM PELLETS AT DIFFERENT RESIDENCE TIMES AND MIR INTENSITIES

At fixed MIR intensity, the thermal conductivity decreases with increasing residence time, until 0.06 W/m/K, and then remains constant. The decrease in thermal conductivity as drying proceeds could be related to the loss of moisture. When the material is wet, the water in the solid must strongly influence the thermal conductivity of the solid.

In order to validate this assumption, the thermal conductivity was plotted versus the pellet moisture content in Figure 26. Prior to drying, the thermal conductivity of the faecal sludge, 0.51 W/m/K, is very similar than that of pure water, 0.58 W/m/K. During drying, the thermal conductivity is directly related to the moisture content, independently from the MIR intensity. Upon reaching a certain point, the thermal conductivity of the solid is not affected anymore by the decrease of moisture in the solid and remains constant. According to Figure 8, this point is when the moisture content is below 40%. The thermal conductivity of the dried solid, which is approximately ten times lower than that of the initial faecal sludge, has a very low value close to usual insulating materials (0.02-0.06 W/m/K) [17].

A low thermal conductivity is an undesirable characteristic for a biofuel, as the resistance for heat penetration within the solid would be more important. The thermal conductivity of diesel, coal and wood (0.1-0.2 W/m/K) is higher than that from dried faecal sludge, except for the thermal conductivity across the grain for some types of wood as balsa (~ 0.055 W/m/K). The thermal conductivity of natural gas (~ 0.03 W/m/K) is lower than the dried pellets, as it could be expected for a gas.

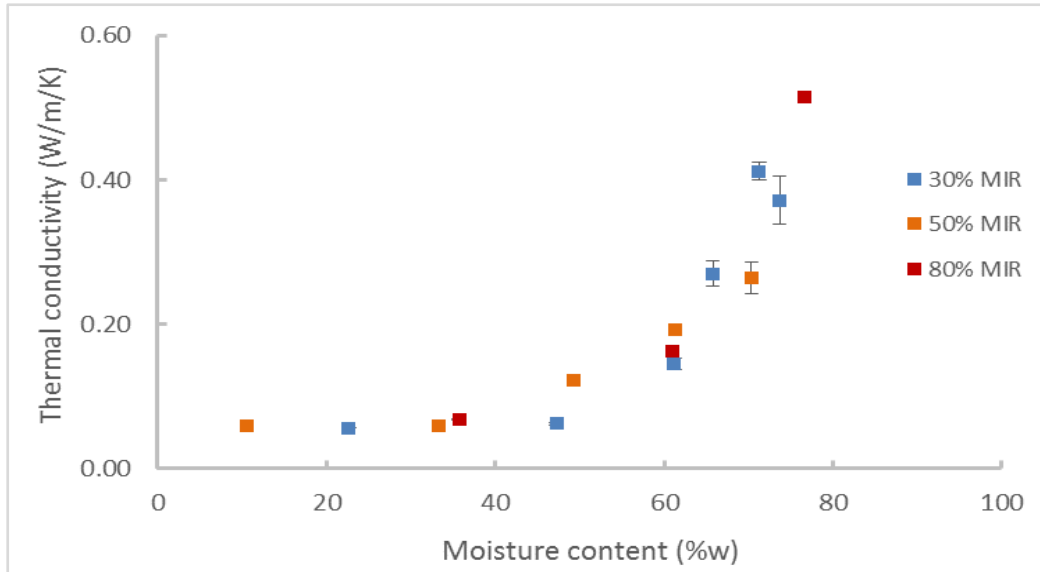


FIGURE 26. THERMAL CONDUCTIVITY VERSUS MOISTURE CONTENT FROM THE 8 MM PELLETS DURING PROCESSING AT DIFFERENT MIR INTENSITIES

### 3.4.2.3 HEAT CAPACITY

The heat capacity of the 8 mm pellets, processed at different MIR intensities and residence time, can be observed in Figure 27.

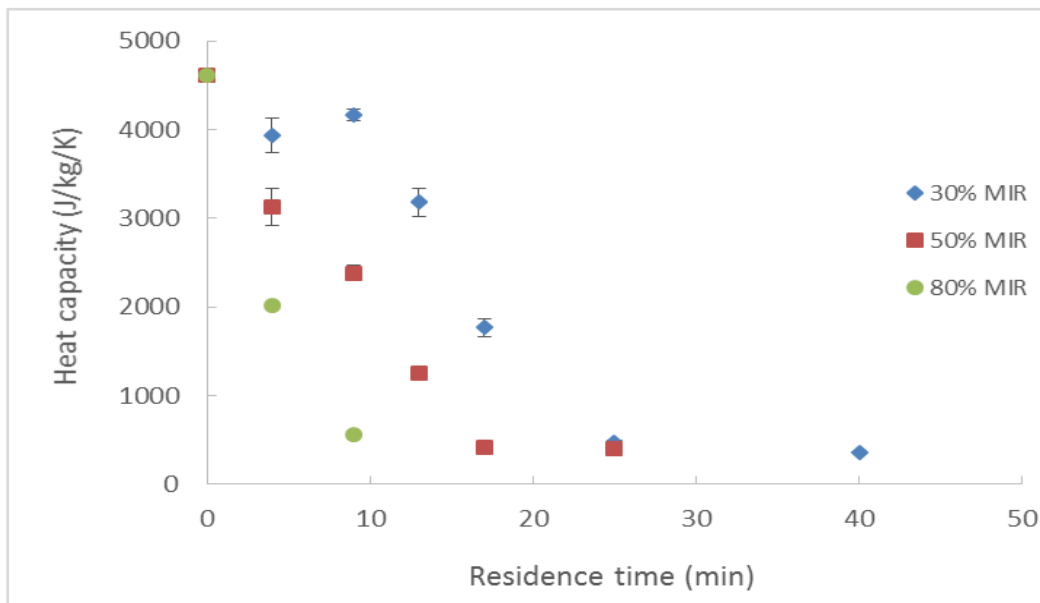
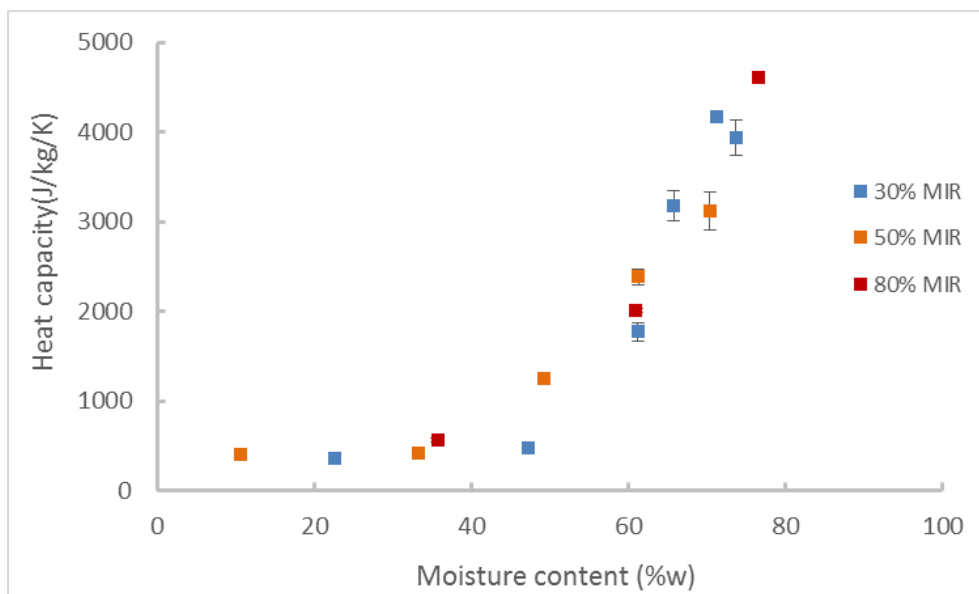


FIGURE 27. HEAT CAPACITY FOR THE 8 MM PELLETS AT DIFFERENT RESIDENCE TIMES AND MIR INTENSITIES

The trend shown by the heat capacity is similar to that observed for the thermal conductivity, i.e. a decrease during drying until arriving at a constant value. This is also due to the decrease in the amount of water in the solid during drying which influences the heat capacity until reaching 40% of moisture content, as seen in Figure 28 which depicts heat capacity versus moisture content. The calorific value of the raw faecal sludge is around 4600 J/kg/K, which is near to the value of pure water, 4187 J/kg/K. The calorific value of the dried sludge is much lower: ~ 400 J/kg/K.

The decrease of heat capacity after drying is positive for any thermal process, as the temperature of the material receiving the heat flux will rise with a lower energy input. This value is much lower than that of other common fuels, e.g. wood, coal, diesel and natural gas (1200-2900 J/kg/K) [18-20].



**FIGURE 28. HEAT CAPACITY VERSUS MOISTURE CONTENT FROM THE 8 MM PELLETS DURING PROCESSING AT DIFFERENT MIR INTENSITIES**

#### 3.4.2.4 THERMAL DIFFUSIVITY

The thermal diffusivity refers to the ability of a body to be heated. It is usually defined as the thermal conductivity divided by the density and the heat capacity.

The thermal diffusivities measured for the 8 mm pellets processed at different residence times and MIR intensity are displayed in Figure 29.

The overall of the thermal diffusivities varies in the range of  $0.9-1.7 \cdot 10^{-7} \text{ m}^2/\text{s}$ . Not a clear trend can be observed for any of the MIR intensities. It only can be noted a slight difference between the dried and wet samples, suggesting an increase of thermal diffusivity during drying. This means that the decrease of heat capacity and density along drying, which is positive for solid heating, is more influent than the decrease of thermal conductivity, which is negative. The heating flux is then more efficiently transferred inside the pellets as the sample is dried.

Compared to other fuels, the thermal diffusivity of dried faecal sludge ( $\sim 1.7 \cdot 10^{-7} \text{ m}^2/\text{s}$ ) is similar to wood and coal ( $\sim 1-2 \cdot 10^{-7} \text{ m}^2/\text{s}$ ), higher than diesel ( $\sim 1.0 \cdot 10^{-7} \text{ m}^2/\text{s}$ ) and lower than natural gas ( $\sim 2.0 \cdot 10^{-5} \text{ m}^2/\text{s}$ ).

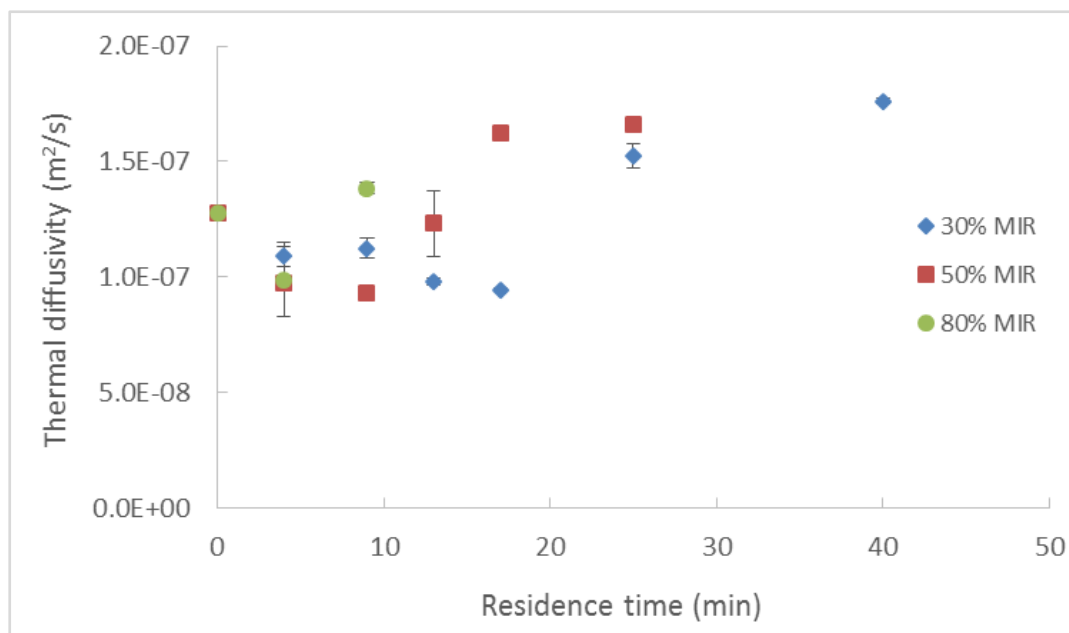


**FIGURE 29. THERMAL DIFFUSIVITY FOR THE 8 MM PELLETS FOR THE 8 MM PELLETS AT DIFFERENT RESIDENCE TIMES AND MIR INTENSITIES**

#### 3.4.2.5 SUMMARY

The dried faecal sludge has a great potential to be used as biofuel: a relatively high calorific capacity, which is similar to wood and some coal ranks; a thermal diffusivity in the same order of magnitude compared to common liquid and solid fuels.

During drying, the loss of water from the solid leads to the decrease of thermal conductivity and heat capacity, until reaching a constant value for moisture contents below 40%. In other words, moisture does not influence pellet thermal properties after removing around 80% of the initial content. The decrease of heat capacity is positive because the pellets would require less energy for their heating. In contrast, the decrease of thermal conductivity is negative as this will increase the resistance for heat transfer within the material. Globally, the positive effect of heat capacity decrease during drying, in addition to the density decrease, is more influent on thermal diffusivity, compared to the negative effect of thermal conductivity decrease. Hence, thermal diffusivity tends to increase as the particle is dried, leading to the improvement of the heating inside the pellets.

In the next chapter, the conclusions of the study are summarised.

## 4. CONCLUSIONS

The main findings of this study can be summarised as following:

- At high MIR emitter intensity (temperatures higher than 200°C), drying occurs the fastest and it is the most efficient, but there is considerable risk of undesirable thermal degradation and burning of the pellets. At medium MIR emitter intensity (temperatures between 100°C and 200°C), the risk of thermal degradation is avoided but drying takes longer. Under these conditions, a residence time of approximately 20 minutes is necessary to reduce the moisture content to 20%. At low MIR intensity (temperatures lower than 100°C), drying is too slow. In all cases, complete pasteurisation is insured in less than 8 minutes.
- The recommended MIR emitter intensity should be the highest one possible without thermal degradation of the pellets. For future work, it is important to determine the temperature and corresponding intensity at which thermal degradation first occurs.
- Minimizing the distance between the emitters and the conveyer belt would lead to energy saving due to lower MIR intensity required to achieve the targeted moisture content and complete pasteurisation.
- Decreasing the pellet size leads to faster drying and a more efficient process.
- Drying rate is slightly faster for faecal sludge without pre-treatment than for a pre-treated sample.
- Drying will be faster by increasing the air flowrate in the heating zone as it will lead to a better evacuation of the evaporated moisture from the surface of the pellets to the environment. However, the air should be heated in order to avoid a cooling effect on particle surface, which has a negative effect on drying rate.
- From a phenomenological point of view, drying occurs in the constant rate period in the early stage and then pellets remain isothermal at the moisture evaporation temperature. After removal of approximately half of the moisture, the drying rate declines, indicating that the pellet surface is fully or partially dried. Therefore, the temperature at the surface increases and becomes considerably higher than at the core. If the heating flux from MIR emitters is too high, the dried surface can be thermally degraded while the core continues to dry.
- Drying provokes some chemical and physical modifications in the pellets: a decrease of the concentration of the soluble nitrogenous compounds, suggesting chemical changes of the nitrogen form in the sample; a decrease in the thermal conductivity and heat capacity, leading to globally a slight increase of the thermal diffusivity. After removing 80% of the initial moisture, these thermal properties attain a stable value.
- The dried pellets present an interesting nutrient composition to be used as an organic fertilizer or soil container. The nutrient content is similar or higher than home compost and manure.
- If the pellets will be used for agricultural purposes, most of the P and N will be slowly released in the soil. A small part of the nitrogen will be fast released, mainly as ammonium. This form is not the most optimal for assimilation by the plants, compared to nitrates, but they can be converted into the latter one by soil microbial activity. The other nutrients, such as K, Mg and Ca, could be expected to be fast released in the soil, as these compounds are soluble in water.
- The use of dried pellets as a biofuel is a potentially interesting alternative, because of the relatively high calorific value and good thermal diffusivity of the material (similar to wood).

## 5. IMPROVEMENTS IN THE FULL SCALE LADEPA

Based on the experimental work and understanding acquired during experiments in the laboratory-scale LaDePa, this section proposes improvements of the full-scale prototype. For this, thermal and mass transfer analysis was performed through calculations, with the objective to improve the transfer phenomena and consequently increase the process efficiency. Otherwise, as the pellets are in contact with the exhaust air from the diesel engine in the pre-heating section from LaDePa machine, the eventual contamination of the material is studied. Finally, a possible design of an optimised LaDePa process is discussed.

### 5.1 THERMAL AND MASS TRANSFER ANALYSIS

The aim of this section is to determine the order of magnitudes of the heating and mass transfer rates. For this, the thermal and mass transfer calculations were simplified as much as possible, accordingly the heating of the pellets was considered to occur without taking into account moisture evaporation latent heat. Hence, the calculations cannot be considered as a precise representation of the reality, but only as rough estimations to get the major trends of the process in terms of transfer phenomena.

Three cases were studied:

- Case 1: the heating rate in the pre-drying section;
- Case 2: the heating rate in the drying zone;
- Case 3: the convective mass transfer rate during drying.

The pellets will be considered as cylinders in the equations. The air stream in the LaDePa machine is considered to contact the pellets in cross flow direction.

#### 5.1.1 HEAT AND MASS TRANSFER CALCULATIONS

##### 5.1.1.1 CONVECTION HEAT TRANSFER CALCULATIONS

The heat transfer by convection at the pellet surface is expressed through Equation 1.

$$c_p \cdot \rho_p \cdot V_p \cdot \frac{\partial T}{\partial t} = \dot{Q}_{conv} \quad \text{Equation 1}$$

With:

$c_p$	heat capacity of the pellets [ $\text{J}\cdot\text{kg}^{-1}$ ]
$\dot{Q}_{conv}$	convective heating rate [W]
$t$	time [s]
$T$	temperature [K]
$V_p$	volume of the pellets [ $\text{m}^3$ ]
$\rho_p$	density of the pellets [ $\text{kg}\cdot\text{m}^{-3}$ ]

The heat of convection is defined by Equation 2.

$$\dot{Q}_{conv} = h_t \cdot S_p \cdot (T_p(t) - T_{air}) \quad \text{Equation 2}$$

With:

$h_t$	thermal transfer coefficient [ $\text{W}\cdot\text{m}^{-2}\cdot\text{K}^{-1}$ ]
$S_p$	surface of the pellets [ $\text{m}^2$ ]

$T_p$  temperature of pellet surface [K]  
 $T_{air}$  temperature of the air stream [K]

The analytical resolution of Equation 1, after combination with Equation 2, leads to Equation 3.

$$\ln\left(\frac{T(t)-T_{air}}{T_i-T_{air}}\right) = -\frac{h_t \cdot S_p}{\rho_p \cdot V_p \cdot Cp_p} \cdot t \quad \text{Equation 3}$$

With:

$T_i$  initial temperature of the pellets [°K]

The heat transfer coefficient can be deduced from the Nusselt number (Equation 4).

$$Nu = \frac{h_t \cdot d_p}{\lambda_p} \quad \text{Equation 4}$$

With:

$d_p$  diameter of the pellet [m]  
 $Nu$  Nusselt number [-]  
 $\lambda_p$  thermal conductivity of the pellet [ $W \cdot m^{-1} \cdot K^{-1}$ ]

The Nusselt number can be calculated using a correlation for cross flow over a cylinder (Equation 5), which is valid for Prandtl values higher than 0.7 and Reynolds values in the range 40-40,000.

$$Nu = 0.683 \cdot Re_p^{0.466} \cdot Pr^{1/3} \quad \text{Equation 5}$$

With:

$Pr$  Prandtl number [-]  
 $Re$  Reynolds number of the particle [-]

The particle Reynolds number is defined by Equation 6.

$$Re_p = \frac{\rho_{air} \cdot d_p \cdot v_{air}}{\mu_{air}} \quad \text{Equation 6}$$

With:

$v_{air}$  velocity of the air stream [ $m \cdot s^{-1}$ ]  
 $\mu_{air}$  viscosity of the air stream [Pa·s]  
 $\rho_{air}$  density of the air stream [ $kg \cdot m^{-3}$ ]

#### 5.1.1.2 CONDUCTION HEAT TRANSFER CALCULATIONS

The heat transfer within a cylinder by conduction was calculated from a heat balance on a solid exposed to transient convective heating (Equation 7).

$$\lambda_p \cdot \frac{1}{r} \cdot \frac{\partial}{\partial r} \left( r \cdot \frac{\partial T}{\partial r} \right) = Cp_p \cdot \rho_p \cdot \frac{\partial T}{\partial t} \quad \text{Equation 7}$$

With:

$r$  position within the pellet [m]  
 $\lambda_p$  thermal conductivity of the pellets [ $\text{K}\cdot\text{m}^{-1}\cdot\text{K}^{-1}$ ]

After a complex mathematical resolution of Equation 7, the temperature at the centre of the cylinder can be expressed by Equation 8.

$$\frac{T_0 - T_{air}}{T_i - T_{air}} = A_1 \cdot e^{-\lambda_1^2 \cdot \tau} \quad \text{Equation 8}$$

With:

$T_0$  temperature at the centre of the pellet [K]  
 $\tau$  dimensionless time [-]

The parameters  $A_1$  and  $\lambda_1$  are coefficients determined from tables as a function of the dimensionless Biot number, which can be expressed as seen in Equation 9.

$$Bi = \frac{h_t \cdot d_p}{4 \cdot \lambda_p} \quad \text{Equation 9}$$

The dimensionless time or Fourier number is determined by Equation 10.

$$\tau = \frac{\alpha_p \cdot t}{r_p^2} \quad \text{Equation 10}$$

With:

$r_p$  radius of the pellets [m]  
 $\alpha_p$  thermal diffusivity of the pellets [ $\text{m}^2 \cdot \text{s}^{-1}$ ]

### 5.1.1.3 RADIATIVE HEAT TRANSFER CALCULATIONS

The radiative heating of the cylinder surface was determined from a heat balance (Equation 11), which also includes the convective effect of the air stream flowing around the solid. The equation was solved numerically by discretisation.

$$C p_p \cdot \rho_p \cdot V_p \cdot \frac{\partial T}{\partial t} = \dot{Q}_{rad} + \dot{Q}_{conv} \quad \text{Equation 11}$$

With:

$\dot{Q}_{rad}$  radiative heating rate [W]

The expression of the radiative heating rate is given by Equation 12, while the expression of the convective heating rate has been already described by Equation 2.

$$\dot{Q}_{rad} = F_{MIR \rightarrow p} \cdot S_p \cdot \sigma \cdot \varepsilon \cdot (T_{MIR}^4 - T_p^4) \quad \text{Equation 12}$$

With:

- $F_{MIR \rightarrow p}$  view factor between the emitters and the pellets [-]
- $T_{MIR}$  temperature of the MIR emitter [K]
- $\sigma$  Boltzmann constant [ $m^2 \cdot kg \cdot s^{-2} \cdot K^{-1}$ ]
- $\varepsilon$  emissivity [-]

The temperature of the radiation source can be deduced from the black body equation (Equation 13).

$$P_{MIR} = S_{MIR} \cdot \sigma \cdot \varepsilon \cdot T_{MIR}^4 \quad \text{Equation 13}$$

With:

- $P_{MIR}$  power emitted by the MIR emitters [W]
- $S_{MIR}$  surface of the MIR emitters [ $m^2$ ]

For simplification, the radiative heating surface density (heating rate of radiation / surface of the body) is assumed to be uniform along the conveyer belt. This implies that the radiation power received per surface area unit is equal between the conveyer belt and the pellets, which leads to equation 14.

$$F_{MIR \rightarrow p} \cdot \sigma \cdot \varepsilon \cdot (T_{belt}^4 - T_p^4) = F_{MIR \rightarrow belt} \cdot \sigma \cdot \varepsilon \cdot (T_{MIR}^4 - T_p^4) \quad \text{Equation 14}$$

With:

- $F_{MIR \rightarrow belt}$  view factor between the emitters and the conveyer belt [-]
- $T_{belt}$  temperature of the conveyer belt [K]

Assuming that the conveyer belt and the pellets are in thermal equilibrium, their temperature are equal, so  $F_{MIR \rightarrow p} = F_{MIR \rightarrow belt}$ . For the calculation of the view factor between the MIR emitters and the conveyer belt, the system was treated as a radiation exchange between two parallel rectangular surfaces. The view factor corresponding to this system is calculated by the equations shown in Figure 30.

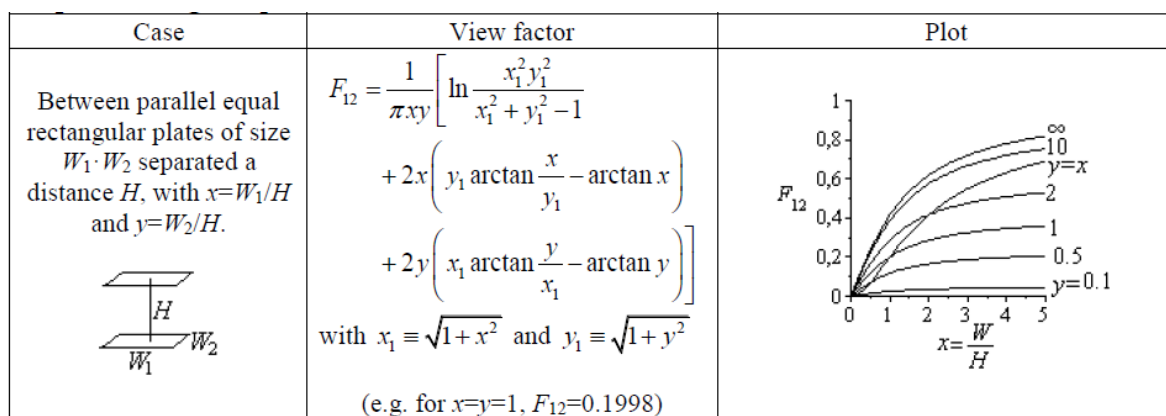


FIGURE 30. EQUATIONS FOR THE CALCULATION OF THE VIEW FACTOR BETWEEN TWO PARALLEL RECTANGULAR SURFACES

## 5.1.1.4 CONVECTIVE MASS TRANSFER CALCULATIONS

The rate of moisture transfer between the pellets and the surrounding air stream is expressed by Equation 15.

$$r_m = h_m \cdot \frac{A_p}{V_p} \cdot (C_{H_2O,p} - C_{H_2O,air}) \quad \text{Equation 15}$$

With:

$C_{H_2O,air}$	moisture concentration in the air stream [mol.m <sup>3</sup> ]
$C_{H_2O,p}$	moisture concentration in the pellet [mol.m <sup>3</sup> ]
$h_m$	convective mass transfer coefficient [m·s <sup>-1</sup> ]
$r_m$	convective mass transfer rate [mol·s <sup>-1</sup> ]

The convective mass transfer coefficient is obtained by combining Equations 16 and 17. The first expression corresponds to the definition of Sherwood number. The second expression corresponds to the Sherwood correlation valid for cross flow over a cylinder, for Prandtl number higher than 0.7 and Reynolds number ranging from 40 to 40,000.

$$Sh = \frac{h_m \cdot d_p}{D_{air-H_2O}} \quad \text{Equation 16}$$

$$Sh = 0.683 \cdot Re_p^{0.466} \cdot Sc^{1/3} \quad \text{Equation 17}$$

With:

$D_{air-H_2O}$	diffusion coefficient of steam into air [mol.m <sup>3</sup> ]
$Sc$	Schmidt number [-]
$Sh$	Sherwood number [-]

## 5.1.2 PARAMETERS USED FOR THE CALCULATIONS

## 5.1.2.1 AIR AND PELLETS PHYSICAL PROPERTIES

Two cases were studied for the air stream used in the LaDePa process. In the first case, the air stream is taken from the ambient, so its temperature is at 20°C. In the second case, the air is issued from the diesel generator, so its temperature is assumed to be at 400°C. The physical properties of air at these two temperatures are shown in Table 8.

TABLE 8. PHYSICAL PROPERTIES OF AIR AT 20°C AND 400°C

	20 °C	400 °C
Viscosity $\mu_{air}$ [Pa·s]	1.821·10 <sup>-5</sup>	3.277·10 <sup>-5</sup>
Density $\rho_{air}$ [kg·m <sup>-3</sup> ]	1.205	0.524
Thermal conductivity $\lambda_{air}$ [W·m <sup>-1</sup> ·K <sup>-1</sup> ]	0.0257	0.0515
Diffusion coefficient $D_{air-H_2O}$ [m <sup>2</sup> ·s <sup>-1</sup> ]	3.0·10 <sup>-5</sup>	-
Prandtl number $Pr$ [-]	0.713	0.680
Schmidt number $Sc$ [-]	0.6	-

Concerning the pellets, two cases were considered: raw faecal sludge (wet material), and processed faecal sludge (dried up to 2 % of moisture content). The physical properties of both cases are presented in Table 9.

**TABLE 9. PHYSICAL PROPERTIES OF THE RAW AND PROCESSED FAECAL SLUDGE**

	<b>Fresh</b>	<b>Dried</b>
<b>Heat capacity <math>C_{p_p}</math> [J·kg<sup>-1</sup>·K<sup>-1</sup>]</b>	4600	400
<b>Density <math>\rho_p</math> [kg·m<sup>-3</sup>]</b>	1100	80
<b>Thermal diffusivity <math>\alpha_p</math> [m<sup>2</sup>·s<sup>-1</sup>]</b>	1.0·10 <sup>-7</sup>	1.7·10 <sup>-7</sup>
<b>Thermal conductivity <math>\lambda_p</math> [W·m<sup>-1</sup>·K<sup>-1</sup>]</b>	0.51	0.06

#### 5.1.2.2 LADEPA DIMENSIONS

The dimensions of the pre-drying and MIR boxes from the full scale LaDePa are summarised in Table 10.

**TABLE 10. DIMENSIONS OF THE DIFFERENT SECTIONS OF THE FULL SCALE LADEPA**

	<b>Length [m]</b>	<b>Large [m]</b>	<b>Height [m]</b>
<b>Pre-drying box</b>	-	1.35	1.2
<b>MIR drying box</b>	5.5	0.95	0.06

As approximation, the length and large of the MIR emitters, the conveyer belt and the suction area are the same than those of the drying zone.

#### 5.1.2.3 LADEPA OPERATING CONDITIONS

The flow rate in the pre-drying and MIR sections in the full scale LaDePa are 1.0 and 3.2 m<sup>3</sup>·s<sup>-1</sup> respectively. The power consumed by the MIR emitters is 144 kW. According to Equation 13, the temperature on the emitter surface is then around 560°C. The pellet diameter and length are of 6 and 50 mm respectively.

### 5.1.3 RESULTS OBTAINED FROM THE CALCULATIONS

#### 5.1.3.1 CASE 1

Case 1 studies the heating of the pellets at the surface and at the centre in the pre-drying section of LaDePa, as if the faecal sludge was fresh or dried. The heat will be provided by the exhaust air from the diesel engine, which is at a temperature of 400°C. The gas flowing across the pellets has a velocity 0.63 m·s<sup>-1</sup> (value obtained after dividing the air flowrate by the cross section area of the pre-drying box), accordingly the particle Reynolds number is of 122. According to the values of the particle Reynolds and Prandtl numbers ( $Sc = 0.7$ ), the use of Equation 5 to determine the heat exchange coefficient is justified (refer to **section 6.1.1.1**). The results from the calculations are depicted in Figure 31.

As expected, the surface of the pellet is heated around 2 times faster compared to the centre for both the fresh and dried faecal sludge. The heating of the pellet is not isothermal in any of the cases and a temperature gradient then exists within the solid. This result agrees with the experimental

observations from the temperature measurements described in **section 3.2.1**. Otherwise, the heating of the dried pellets is around 10 times faster than that from the fresh sample. This result must be related to the higher thermal diffusivity measured for dried faecal sludge compared to the value found for the fresh material (**section 3.3.2.4**).

The time required to heat the pellet surface up to the water evaporation temperature, i.e. 100°C, is of 7 and 60 s for the dry and fresh faecal sludge respectively. The time taken to the centre of the pellet to attain this temperature is 14 s and 140 s for the dry and fresh faecal sludge respectively. It can be seen that the time required to heat the entire pellet body up to 100°C is lower than the residence time in the pre-drying zone, i.e. 240 s. Consequently, the pellets are theoretically able to attain the water evaporation temperature in the pre-drying zone.

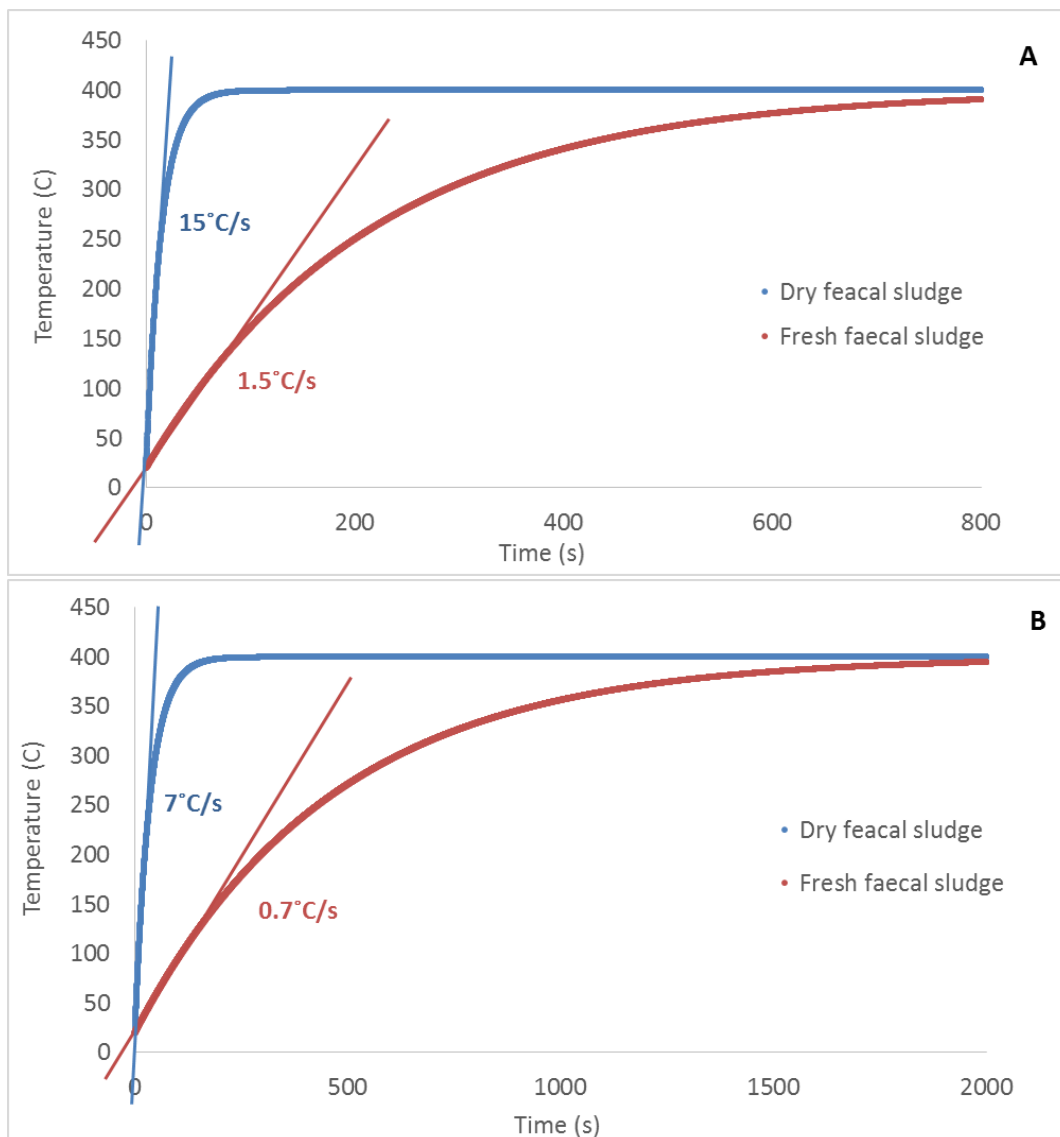


**FIGURE 31. TEMPERATURE OF THE FRESH AND DRY FAECAL SLUDGE AT THE SURFACE (A) AND AT THE CENTRE (B)**

## 5.1.3.2 CASE 2

The heating of the pellets at the surface in the MIR section was studied for three different situations. The first situation corresponds to the current operating mode of LaDePa machine, where the carrier gas is directly issued from the ambient air. The carrier gas is then considered to be at a temperature of 20°C and at a velocity of 0.6 m·s<sup>-1</sup> (value obtained after dividing the air flowrate by the suction surface area). The second situation occurs similarly to the first one but the air stream is previously heated up to 400°C before introduction into the heating zone. In the third situation, the carrier air is again pre-heated at 400°C and the suction section area is reduced by a factor of 5, leading to the increase of the air velocity to 2.4 m·s<sup>-1</sup>.

The first aspect to study was the relationship of the factor of view with respect to the distance between the MIR and the pellets, which was done in Figure 32. The factor of view here refers to the total radiation received by the body to heat with respect to the total radiation emitted by the source. When the view of factor tends to 1, the radiation emitted by the MIR emitters is entirely received by the pellets. When the view of factor is lower than 1, part of the MIR radiation is not received by the pellets and is then lost in the surroundings. The part of lost radiation increases as the view of factor decreases. For distances between the MIR emitter and the pellets lower than 0.08 m, the view of factor is close to 1. Above this distance, the view of factor is lower than 0.9, and so the loss of radiation starts to be considerable. In the studied case, the pellets are distanced of 0.06 m with respect to the MIR emitters, which represents a factor of view of 0.93. Most of the radiation emitted by the source is then received by the pellets.

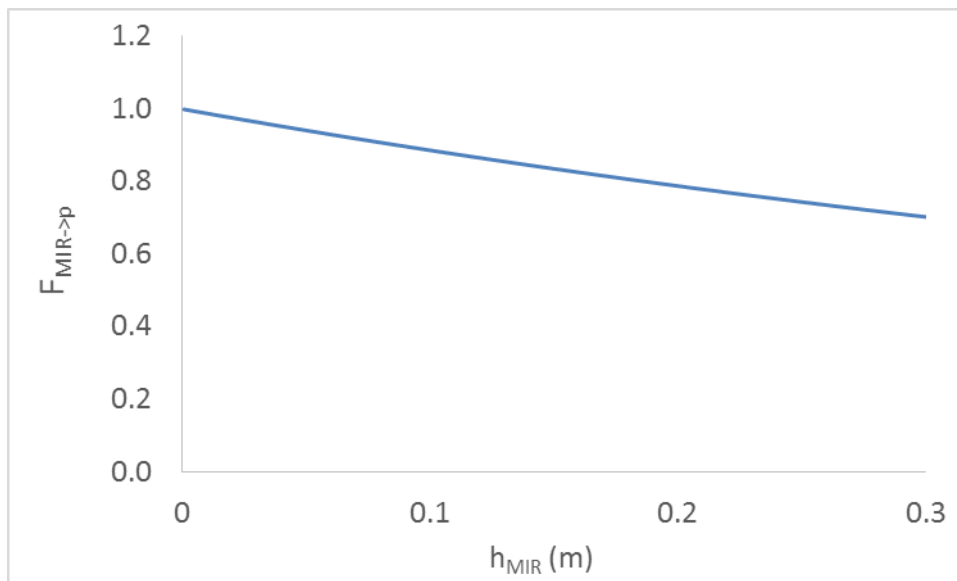
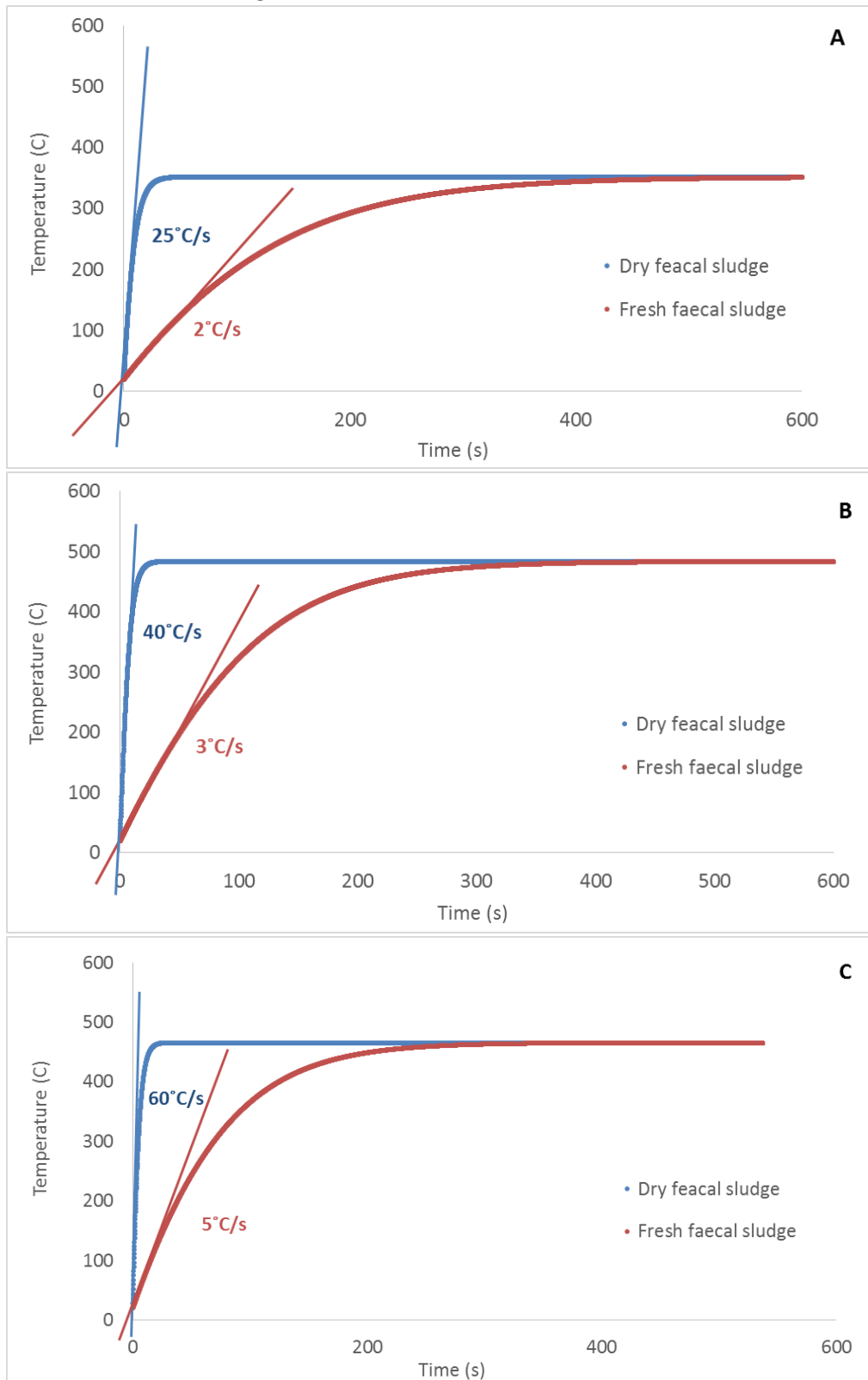


FIGURE 32. VIEW OF FACTOR VERSUS THE DISTANCE BETWEEN THE MIR AND THE CONVEYER BELT

Figure 33 shows the temperature at the pellet surface for each of the different situations which were tested in this section. The MIR intensity is set to 115 kW, which corresponds to a temperature of 515°C at the emittance surface. The gas velocities of 0.6 and 2.4 m·s<sup>-1</sup> lead to respective particle Reynolds numbers of 220 and 1765. Both cases are comprised in the validity range for the use of Equation 5 to calculate the heat transfer coefficient. The faecal sludge was considered as fresh and dried for the calculations, without previous pre-heating. The temperature at the pellet centre is not included in the

analysis, as the internal heating is assumed to occur similarly compared to case 1, i.e. two times slower than the external heating.



**FIGURE 33. TEMPERATURE AT THE PELLET SURFACE IN THE MIR HEATING ZONE – (A) CARRIER GAS AT AMBIENT TEMPERATURE; (B) CARRIER GAS PRE-HEATED TO 400°C; (C) CARRIER GAS PRE-HEATED TO 400°C AND SUCTION SECTION AREA REDUCED BY A FACTOR OF 5**

The dried pellets are heated faster than the fresh material by a factor of approximately 10, as also found in case 1. It also can be seen that the heating rate is increased by pre-heating the carrier gas and / or by reducing the suction surface area. Indeed, pre-heating the carrier gas avoids a cooling effect on the pellet as if air at ambient temperature was introduced in the MIR section. Moreover, the reduction of the suction area leads to higher air velocities so that the convective heating contribution is increased.

The time required to reach 100°C for the dry and fresh faecal sludge is respectively: 4 and 50 s with the actual LaDePa operating mode; 2.5 and 33 s by preheating the gas; 1.5 and 20 s by preheating the gas and reducing the suction section area. As the residence time in the drying chamber is usually set to 240 s, there is theoretically enough time for the pellets to reach the temperature of water evaporation.

#### 5.1.3.3 CASE 3

As expressed in Equation 15, the mass transfer of the evaporated moisture from the pellet surface to the surroundings is driven by the difference of water content between the solid and the environment. In the LaDePa drying chamber, the carrier air is charged with the ambient moisture and the moisture issued from faecal sludge drying. In Durban, the annual mean temperature is 20 °C with 80% of relative humidity, which leads to a moisture concentration of 0.014 kg·m<sup>-3</sup>. The typical faecal sludge feed rate in LaDePa is set to 850 kg·h<sup>-1</sup> and the final product usually attains 20% of moisture content. The moisture removal rate is then 680 kg·h<sup>-1</sup> (0.189 kg·s<sup>-1</sup>), corresponding to a moisture concentration of 0.059 kg·m<sup>-3</sup> in the carrier air. By summing the moisture from the environment and the process, the moisture concentration in the carrier air can attain a value of 0.073 kg·m<sup>-3</sup>. Considering that 20% of moisture content remains in the dried pellets, the concentration in the solid is 176 kg·m<sup>-3</sup>. It can be clearly seen that the concentration in the pellets is significantly higher than that in the carrier gas, which can be consequently neglected. At lower degree of drying, the difference of moisture concentration between the solid and the carrier gas is even higher. It can be then concluded that the moisture in the carrier gas is not influencing during pellets drying.

The external mass transfer rate was calculated for two different suction section areas: one corresponding to the actual LaDePa configuration, and the other to the suction area reduced by a factor of 5. The mass transfer rates are respectively 0.59 and 1.26 kg·h<sup>-1</sup>. As it could be expected, the decrease of the suction area leads to faster mass transfer, as the air carrier velocity is increased.

#### 5.1.4 SUMMARY

The thermal and mass transfer calculations performed in this section support the experimental observations presented in the previous sections. It has been demonstrated that the heating of the pellets is not isothermal, and that the dried faecal sludge is more rapidly heated compared to the fresh material. In the actual configuration of LaDePa, the time required to heat the pellets seems large enough with respect to the residence time. Nonetheless, the operating conditions can be largely improved in the MIR section, which would result in a lower power consumption and in a consequent decrease of operating costs. Particularly, the air suction section could be optimised: the suction area could be reduced in order to lead to higher air velocities and consequently to higher heat and mass transfer rates; the carrier air could be pre-heated in order to increase the heat input for moisture

evaporation. Moreover, the distance between the belt and the emitters should be reduced up to a few cm in order to maximise the radiation received by the belt.

## 5.2 PELLET CONTAMINATION BY THE EXHAUST GAS FROM THE DIESEL ENGINE

The electricity in the LaDePa process is provided by a diesel generator. The heat from diesel combustion is employed in the pre-drying section of the process by putting into direct contact the pellets with the exhaust air flow. However, this practice can cause the contamination of the pellets by undesirable compounds from diesel combustion.

Figure 34 shows a typical composition of diesel fuel. It can be noticed that diesel includes several trace elements which can be highly toxic for biological organisms such as: Cadmium (Cd), Cobalt (Co), Chromium (Cr), Nickel (Ni), Lead (Pb), Thallium (Ti). The adsorption of these elements on the pellets could pose a human and environmental hazard problem for their reuse in agriculture, as the soil and the crops would be potentially contaminated by these elements. Additionally, the underground water would also risk to result contaminated in the long term.

The combustion of diesel can also provoke the formation of environmental hazardous compounds as polycyclic aromatic hydrocarbons and soot particles. The typical exhaust gas composition from Diesel combustion is displayed in Figure 35.

<b>C</b>	87.4 wt%					<b>Cd</b>	0.525 mg/l
<b>H</b>	12.1 wt%					<b>Co</b>	2.046 mg/l
<b>N</b>	392 wt ppm					<b>Cr</b>	4.4 mg/l
	140 wt ppm					<b>Cu</b>	2.78 mg/l
<b>S</b>	1.39 wt ppm					<b>Mn</b>	1.04 mg/l
	0.037 wt ppm					<b>Mo</b>	4.27 mg/l
<b>Al</b>	32.8 mg/l					<b>Ni</b>	2.61 mg/l
<b>Ca</b>	41.2 mg/l					<b>Pb</b>	2.04 mg/l
<b>Fe</b>	27.8 mg/l					<b>Sb</b>	0.973 mg/l
<b>Mg</b>	7.12 mg/l					<b>Sr</b>	0.713 mg/l
<b>Si</b>	46 mg/l					<b>Ti</b>	4.07 mg/l
<b>Ag</b>	0.707 mg/l					<b>V</b>	1.03 mg/l
<b>Ba</b>	1.12 mg/l					<b>Zn</b>	5.63 mg/l

FIGURE 34. TYPICAL DIESEL COMPOSITION [21, 22]

O <sub>2</sub>	12.5 %		[10-15]	
CO <sub>2</sub>	7 wt%		[7]	
H <sub>2</sub> O	4.2 wt%		[1.4 - 7]	
CO	750 wt ppm		[300 - 1200]	
NO <sub>x</sub>	625 wt ppm		[350 - 1000]	
HC	190 wt ppm		[50 - 330]	
H <sub>2</sub>	250 wt ppm		[100 - 400]	
SO <sub>x</sub>	55 wt ppm		[10 - 100]	
Particules	65 mg/m <sup>3</sup>		[65]	
N <sub>2</sub>	76.3 wt%			
These results were obtained for :			$m_{\text{diesel}} / m_{\text{O}_2}$	26

FIGURE 35. TYPICAL EXHAUST GAS COMPOSITION FROM DIESEL COMBUSTION [23]

The contamination potential of the pellets with hazardous elements is in the order of mg/kg concerning hydrocarbons and particulates, and 0.01 mg/kg for the inorganic elements. These concentrations are low but their effects after accumulation and exposure at long term are uncertain in the case of reuse of the contaminated pellets in agriculture.

In order to elude the risk of pellets contamination, it would be suitable to avoid the direct contact of the pellets with the exhaust air in the pre-drying chamber of LaDePa. As a solution, heat exchangers could be employed in order to transfer the heat from the exhaust combustion gas to an ambient air stream which presents no risks.

### 5.3 IMPROVEMENT OF LADEPA DESIGN

From the experimental work and calculations conducted in this study, a new improved design of LaDePa machine is here proposed. The principle is basically the same than the current process, with some technical changes and modifications in the operating mode.

The main feature of the new LaDePa design is to process faecal sludge into a high heating intensity stage followed by a mild heating stage. To achieve this, the MIR section is split into two distinct sections with different emitter intensity. The pre-drying section is removed as it is unnecessary. In fact, the fresh faecal sludge has a high resistance to heat penetration, so it is more suitable to combine the MIR and convective heating from the beginning of heating. The carrier air in the drying section will be extracted from the environment and divided into two streams. Each of the streams will be heated by the hot exhaust gas issued from the diesel engine up to a temperature suitable for the drying section where it will be introduced. Indeed, the carrier air in the high heating intensity stage should

have an enough high temperature, whereas temperature should be lower for the mild heating intensity stage. At the outlet of LaDePa, the pellets will be collected in a thermal insulated container with eventual heating using residual heat from the process. The aim will be to maintain elevated the temperature of the pellets as long as possible to ensure pasteurisation.

In the high heating intensity stage, the heat provided by the MIR emitters and the air carrier stream should lead to temperatures higher than 220°C inside the chamber. The high heat input should enhance fast drying rates. In this section, drying should occur in the constant rate period, where kinetics are controlled by external factors. Thus, the air carrier velocities should be imperatively as high as possible in order to maximise the drying rate. As the pellets surface is supposed to remain wet during the constant rate period, the body temperature is controlled by moisture evaporation at around 100°C, which consequently avoids undesirable thermal degradation. In the mild heating intensity stage, the heat input from the MIR emitters and the air carrier stream is reduced so that the pellet surface is not thermally damaged after drying. The optimum temperature inside this section is near 180°C, where the drying rate is maximised without the risk of thermal degradation. The target of this stage is to dry the interior of the pellets and achieve pathogens deactivation.

According to the experiments in the laboratory-scale LaDePa, the transition between the two drying stages must occur before the pellets attain 60% of moisture content, i.e. after removing approximately half of the initial moisture. At the high heating intensity, the moisture content can be lowered up to 50% after 4 minutes of residence time. At medium heating intensity, moisture content at 60% is removed up to 20% after 10 minutes of residence time or up to 10% after 15 minutes. These values are only indicative for the full-scale prototype where the residence time should be shorter due to the higher air carrier temperature and velocities, and the lower pellet size (6 mm) employed in the real process.

Figure 36 proposes a diagram flow sheet of an improved LaDePa process. The temperature is merely indicative. In this diagram, two successive heat exchangers are used to heat the air carrier streams. The first heat exchanger allows to transfer major part of the heat from the diesel combustion exhaust gas to the air stream to introduce into the high heating chamber. In the second heat exchanger, the residual heat from the exhaust gas is employed to heat the carrier air to introduce into the mild heating chamber and the pellets collecting containers. This configuration is only a possibility among others. For instance, a single heat exchanger could be employed for the air carrier heating and then the different streams will be mixed with ambient air so as to obtain the desired temperature.

Among further innovations, a crusher could be installed in the LaDePa machine, after the pellets have obtained a minimal moisture content so as to be easily grindable. The crusher will reduce the size of the pellets into fine particles which will continue to be heated in order to reach lower moisture contents and ensure pasteurisation. As the size of the faecal sludge will be reduced, the heat and mass transfer will occur in a more efficient way, lowering the heating requirements of the material. By using a crusher with low energetic requirements, the operation cost of the plant could be reduced due to the energy savings from the heating section after grinding the pellets. At the end, the particles could be agglomerated into dense pellets to be used in agriculture or as a biofuel.

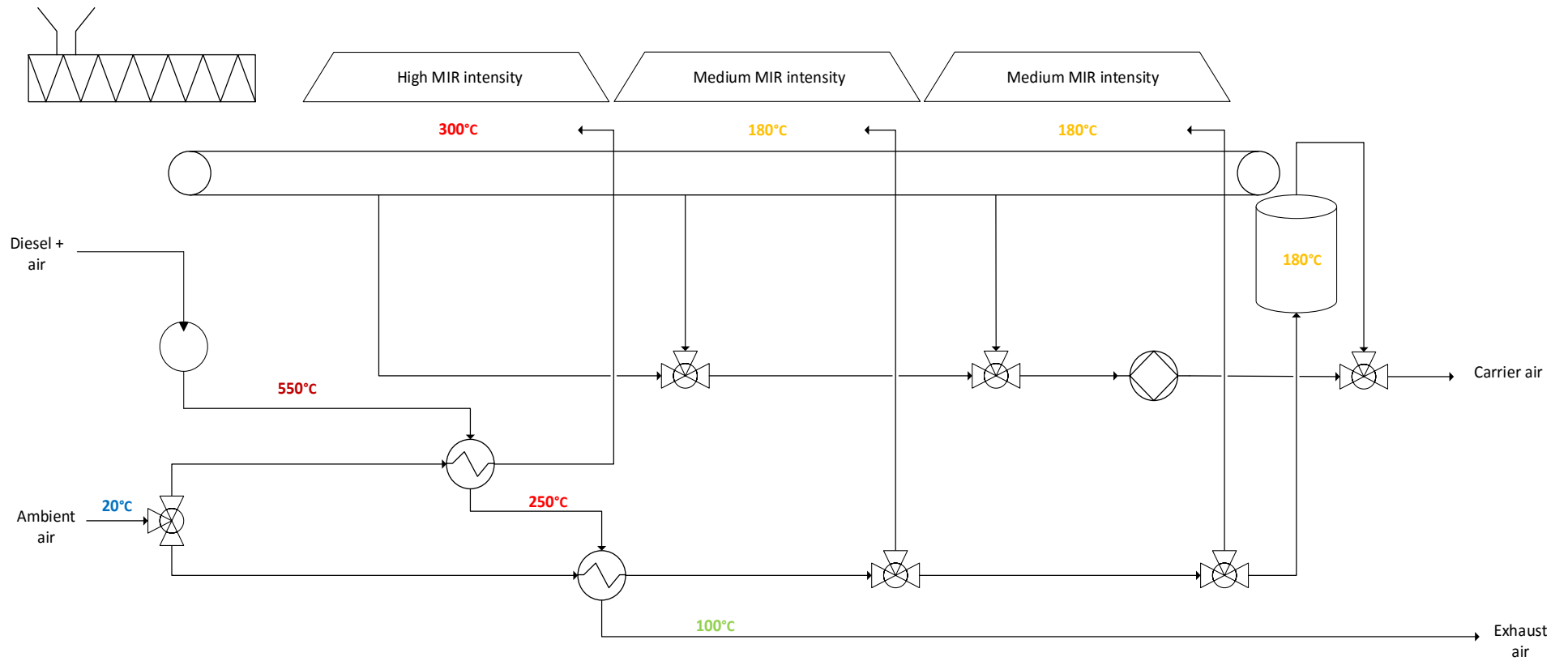


FIGURE 36. DIAGRAM FLOW SHEET OF THE IMPROVED LADEPA DESIGN

## 6. LIST OF PUBLICATIONS

S.W. Mirara, S. Santiago, A. Singh, K. Velkushanova, C.A. Buckley. *Pasteurisation and drying of faecal sludge by use of wave medium infrared (MIR) radiation*. Poster FSM III Conf., Hanoi, Vietnam: 2015.

S. Septien, A. Singh, S.W. Mirara, L. Teba, K. Velkushanova, C.A. Buckley. *Overview of 'LaDePa' Process, for Drying and Pasteurisation of Faecal Sludge from VIP latrines using IR Radiation*. 4<sup>th</sup> YWP-ZA Biennial and 1<sup>st</sup> African YWP Conf., Pretoria, South Africa: 2015.

S.W. Mirara. *Drying and pasteurisation of faecal sludge from VIP latrines using a pilot scale LaDePa process*. M<sub>eng</sub> thesis: 2016.

S. Septien, S.W. Mirara, A. Singh, K. Velkushanova, C.A. Buckley. *Use of 'LaDePa' process for the drying and pasteurisation of faecal sludge from VIP latrines by the means of infrared radiation*. Under redaction, to be published in Water Science and Technology.

S.W. Mirara, S. Septien, A. Singh, K. Velkushanova, C.A. Buckley. *Characterisation of a drying and pasteurisation process, 'LaDePa', for the treatment of faecal sludge*. Under redaction, to be published in Chemical Engineering Journal.

## 7. CAPACITY BUILDING

The table below presents a list of under-graduate and post-graduate students involved in this research (Volume 2: K5/2137).

Type	Name	Gender	Nationality	Race	Actual degree
<b>M<sub>eng</sub> student</b>	S.W. Mirara	Male	Kenyan	Black	M <sub>eng</sub> (2016)
<b>B<sub>eng</sub> student</b>	N. Moodley	Female	South African	Indian	B <sub>eng</sub>
<b>B<sub>eng</sub> student</b>	R. Gengiah	Female	South African	Indian	B <sub>eng</sub>
<b>B<sub>eng</sub> student</b>	M. Patel	Male	South African	Indian	B <sub>eng</sub>
<b>B<sub>eng</sub> student</b>	T. Hlongwane	Female	South African	Black	B <sub>eng</sub>
<b>Post-doctorate</b>	S. Septien	Male	Mexican	Latin	PhD
<b>Lecturer</b>	A. Singh	Female	South African	Indian	M <sub>eng</sub>

## 8. REFERENCES

- [1] Dhib, R. Infrared Drying: From Process Modeling to Advanced Process Control. *Dry Technol* 2007;25:97-105.
- [2] Navarri, P., Andrieu, J., Gevaudan, A. Studies on infrared and convective drying of non hygroscopic solids. In: Mujumdar, A.S., editors. *Dry. '92*. Mujumdar, , Amsterdam: Elsevier; 1992, p. 685-94.
- [3] Lescanne, Y. Caratérisation du papier en vue de la simulation du séchage par infrarouge électrique. PhD thesis, Institut National Polytechnique de Lorraine, 1992.
- [4] Ghaly, A.E., MacDonald, K.N. Drying of poultry manure for use as animal feed. *Am J Agric Biol Sci* 2012;7:239-54.
- [5] Dail, W.H., He, Z., Erich, Susan M., Honeycutt, Wayne C. Effect of Drying on Phosphorus Distribution in Poultry Manure. *Commun Soil Sci Plant Anal* 2007;38:1879-95.
- [6] Ghadernejad, K., Kianmehr, M.H. Effect of moisture content and particle size on energy consumption for dairy cattle manure pellets. *Agric Eng Int CIGR J* 2012;14:125-30.
- [7] Ghaly, A.E., MacDonald, K.N. Kinetics of thin layer drying of poultry manure. *Am J Biochem Biotechnol* 2012;8:128-42.
- [8] Cotana, F., Coccia, V., Petrozzi, A., Cavalaglio, G., Gelosia, M., Merico, M.C. Energy valorization of poultry manure in a thermal power plant: Experimental campaign. *Energy Procedia* 2014;45:315-22.
- [9] Lundgren, J., Pettersson, E. Combustion of horse manure for heat production. *Bioresour Technol* 2009;100:3121-6.
- [10] Billen, P., Costa, J., Van der Aa, L., Van Caneghem, J., Vandecasteele, C. Electricity from poultry manure: a cleaner alternative to direct land application. *J Clean Prod* 2014.
- [11] Bennamoun, L., Arlabosse, P., Léonard, A. Review on fundamental aspect of application of drying process to wastewater sludge. *Renew Sustain Energy Rev* 2013;28:29-43.
- [12] Ecochem. MANURE IS AN EXCELLENT FERTILIZER 2014. [http://www.ecochem.com/t\\_manure\\_fert.html](http://www.ecochem.com/t_manure_fert.html).
- [13] Harrison, J. NPK Nutritional Values of Animal Manures & Compost, Etc. 2014. <http://www.allotment-garden.org/compost-fertiliser/npk-manures-compost.php>.
- [14] Cuevas, V.C. Rapid Composting Technology in the Philippines: Its Role in Producing Good-Quality Organic Fertilizers. Institute of Biological Sciences, University of the Philippines, Laguna, Philippines: 1997.
- [15] Chemicalland21. NPK, Fertilizer 2013. <http://chemicalland21.com/industrialchem/inorganic/NPK.htm>.

- [16] EngineeringToolBox. Fuels – Higher Calorific Values 2015. [http://www.engineeringtoolbox.com/fuels-higher-calorific-values-d\\_169.html](http://www.engineeringtoolbox.com/fuels-higher-calorific-values-d_169.html).
- [17] FAO. Thermal insulation materials, technical characteristics and selection criteria 2015. <http://www.fao.org/docrep/006/y5013e/y5013e08.htm>.
- [18] EngineeringToolBox. Solids – Specific Heats n.d. [http://www.engineeringtoolbox.com/specific-heat-solids-d\\_154.html](http://www.engineeringtoolbox.com/specific-heat-solids-d_154.html).
- [19] MatBase. Fuels: Natural gas (North Sea) 2015. <http://www.matbase.com/material-categories/other-materials/fuels/material-properties-of-natural-gas-north-sea.html#properties>.
- [20] MatBase. Fuels: Diesel 2015. <http://www.matbase.com/material-categories/other-materials/fuels/material-properties-of-diesel.html#properties>.
- [21] Wang, Y-F., Huang, K-L., Li, C-T., Mi, H-H., Luo, J-H., Tsai, P-J. Emissions of fuel metals content from a diesel vehicle engine. *Atmos Environ* 2003;37:4637-43.
- [22] Hughey, C.A., Hendrickson, C.L., Rodgers, R.P., Marshall, A.G. Elemental Composition Analysis of Processed and Unprocessed Diesel Fuel by Electrospray Ionization Fourier Transform Ion Cyclotron Resonance Mass Spectrometry. *Energy & Fuels* 2001;15:1186-93.
- [23] Kašpar, J., Fornasiero, P., Hickey, N. Automotive catalytic converters: current status and some perspectives. *Catal Today* 2003;77:419-49.

## APPENDIX 1: RHEOLOGICAL CHARACTERISATION OF THE VIP FEACAL SLUDGE

Viscosity of sludge at different shear rate was investigated in a rheometer Anton Parr MCR51 for the VIP faecal sludge with and without sawdust. The rheological curves are presented in Figure A.1.

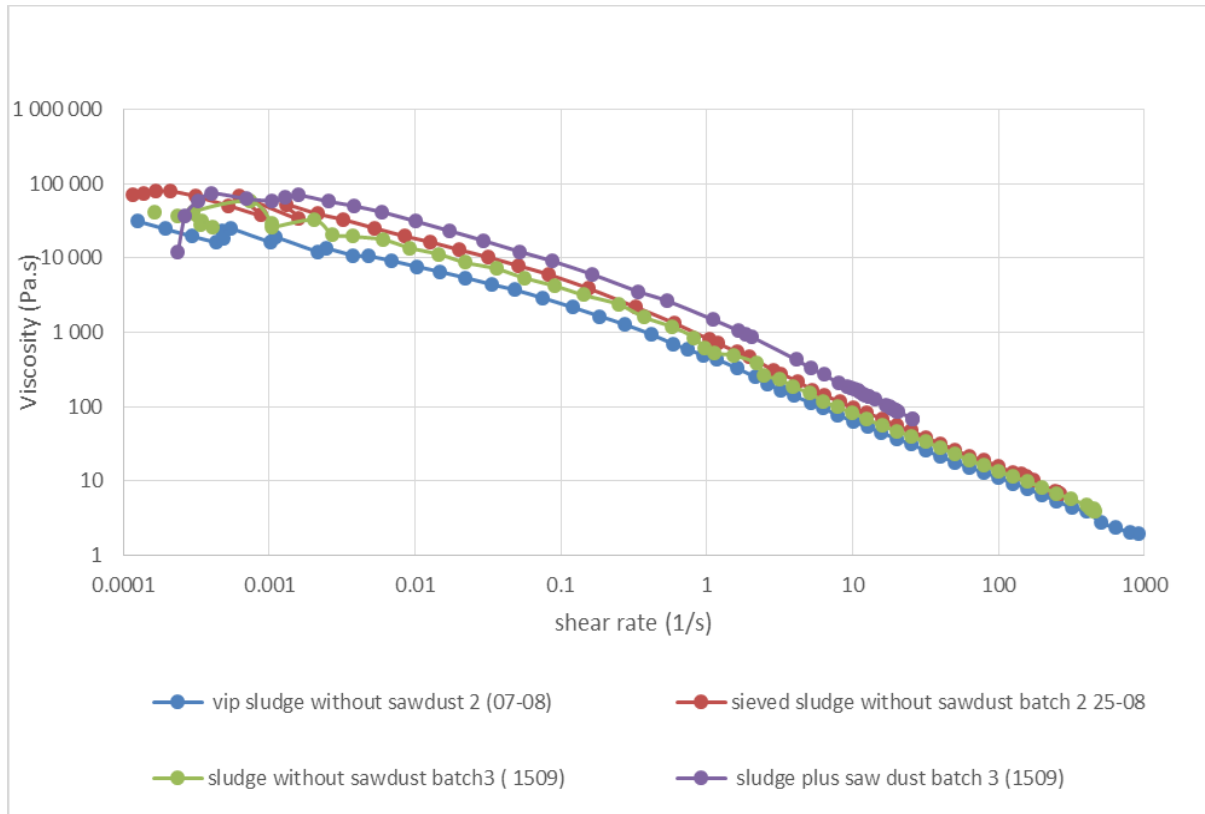
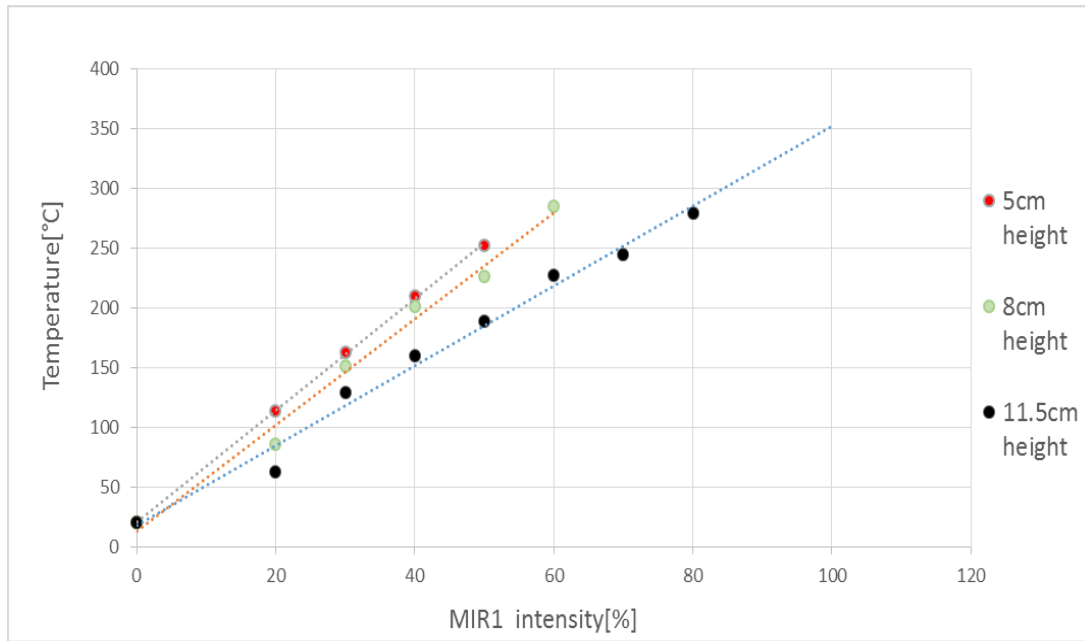


FIGURE A.1. RHEOLOGICAL CURVES FOR THE RAW FAECAL SLUDGE WITH AND WITHOUT THE ADDITION OF SAWDUST

## APPENDIX 2: TEMPERATURE MEASUREMENT DATA

Temperature in the heating zone, measured with the k-type thermocouple at different emitter height above the belt and MIR intensities, is given in Figure B.1 and **Figure B.2** for respectively the first and second emitter. It can be seen that the same temperature can be obtained by different combinations of MIR intensity and emitter height.



**FIGURE B.1. TEMPERATURE MEASURED UNDER THE FIRST MIR EMITTER AT DIFFERENT MIR INTENSITIES AND EMITTER HEIGHTS**

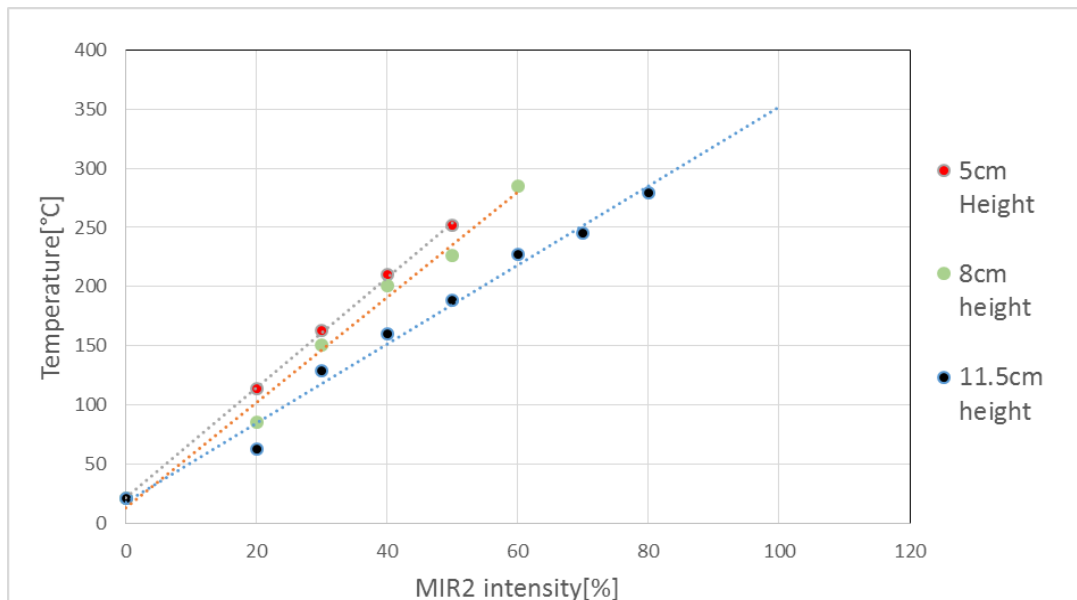


**Figure B.2. Temperature measured under the second MIR emitter at different MIR intensities and emitter heights**

## APPENDIX 3: EFFECT OF PARTICLE SIZE AND AIR FLOWRATE ON THE POTASSIUM AND PHOSPHOROUS COMPOSITION OF THE PELLETS

Figure C.1 and Figure C.2 show the concentration of respectively K and P in pellets of different sizes. In Figure C.3, the concentration of K in the 8 mm pellets processed at two different flowrates (with half open and fully open valve) is shown in Figure C.3.

It can be seen that neither the pellet size nor the air flowrate have an influence on the K and P contents. Some outliers could be observed for the P concentration in the 10 mm and 12 mm pellets. However, these measurements are not enough significant as they have been done once, without any repetition. Anyway, the outliers seem to be more likely attributed to the dispersion of the experimental measurements than to a real difference. More measurements would be required to confirm or deny such assumption.

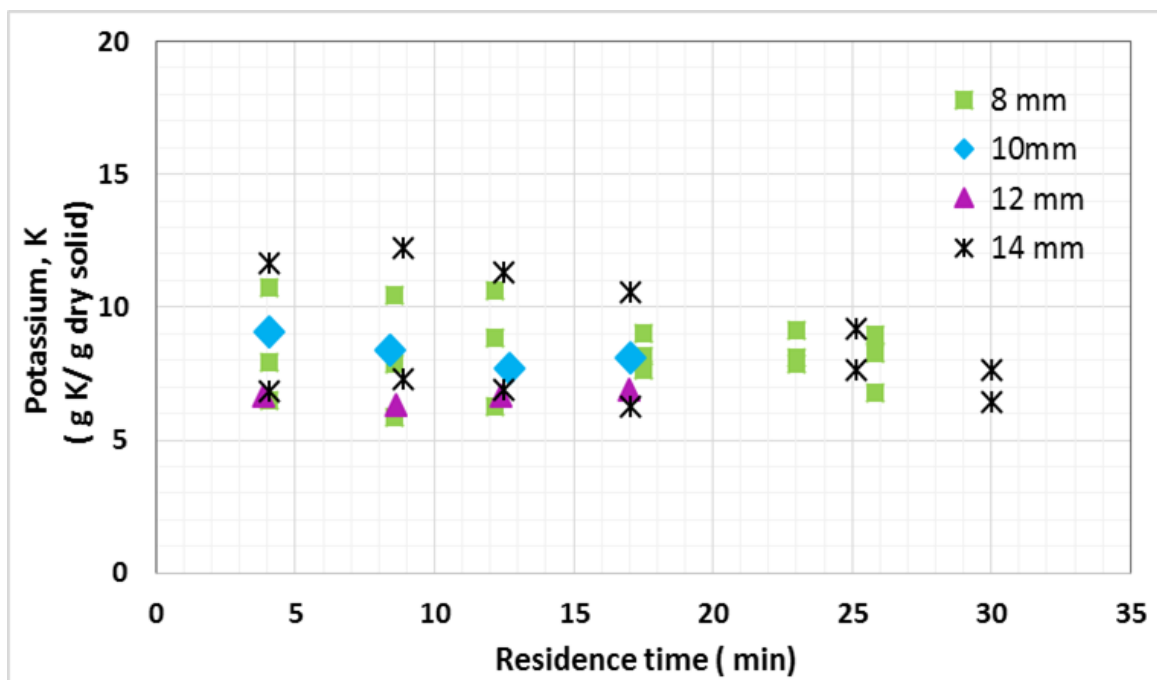


FIGURE C.1. CONCENTRATION OF K IN THE 8 MM, 10 MM, 12 MM AND 14 MM PELLETS PROCESSED AT DIFFERENT RESIDENCE TIMES

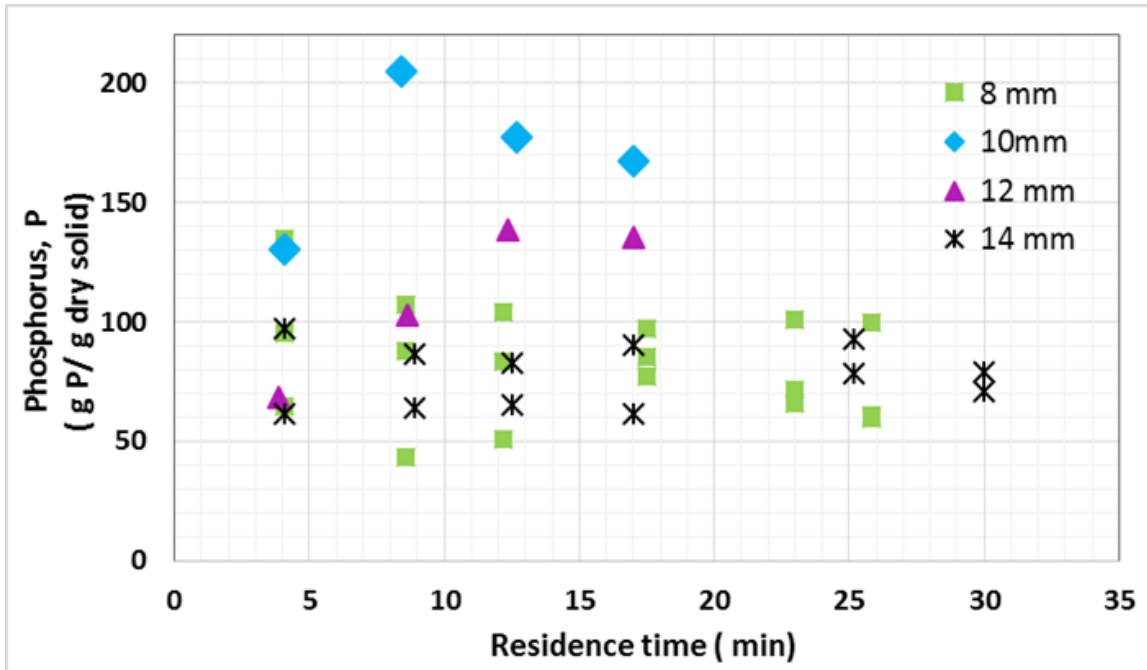


FIGURE C.2. CONCENTRATION OF P IN THE 8 MM, 10 MM, 12 MM AND 14 MM PELLETS PROCESSED AT DIFFERENT RESIDENCE TIMES

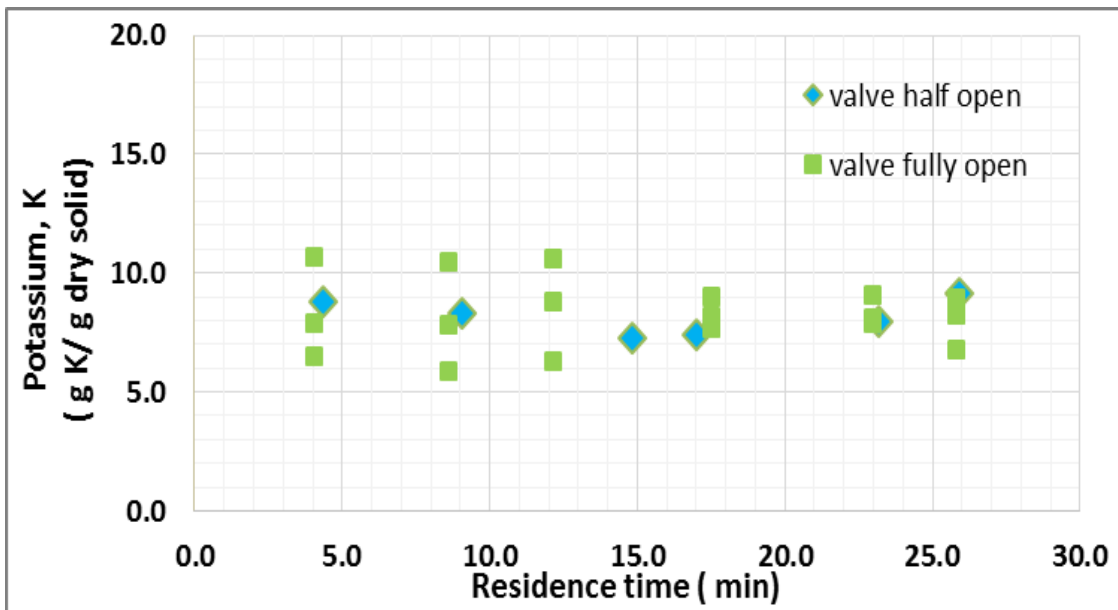


FIGURE C.3. CONCENTRATION OF K IN THE 8 MM PELLETS PROCESSED AT DIFFERENT AIR FLOWRATES AND RESIDENCE TIMES

## APPENDIX 4: EFFECT OF PARTICLE SIZE AND AIR FLOWRATE ON THE CALORIFIC VALUE

The calorific values of pellets of different sizes are displayed in Figure C.2. No considerable differences are observed between the different samples.

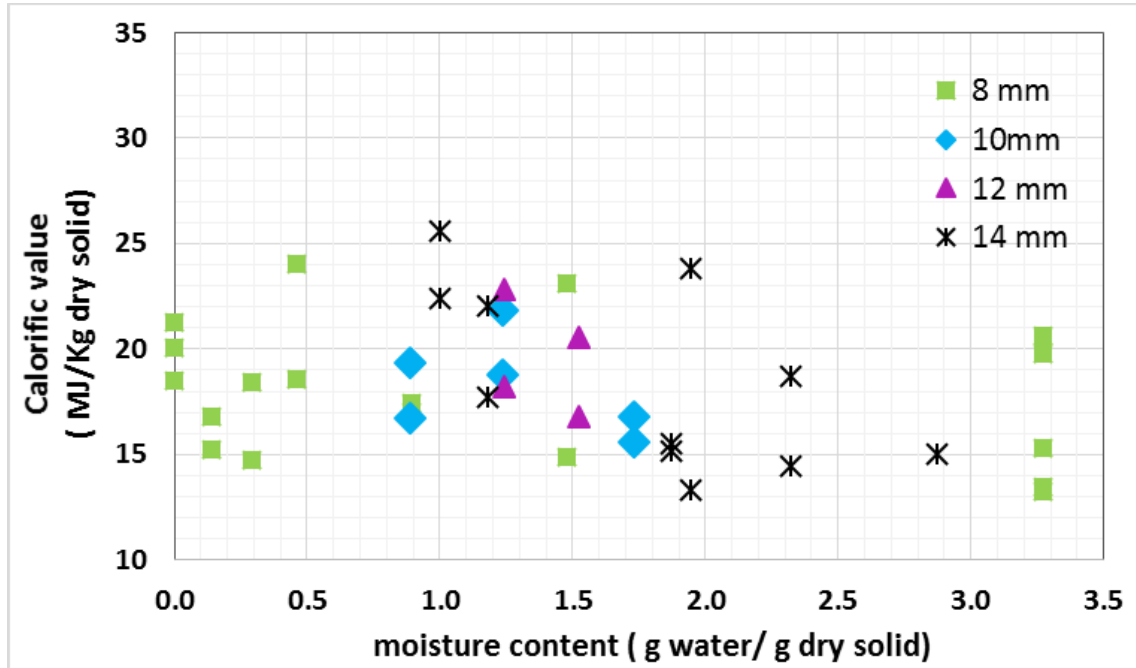


FIGURE D.1. HEAT CAPACITY OF THE 8 MM, 10 MM, 12 MM AND 14 MM PELLETS PROCESSED AT DIFFERENT RESIDENCE TIMES